Journal Pre-proofs

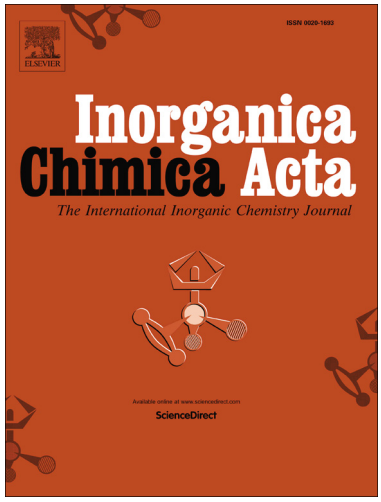

Research paper

Simple salicylaldimine-functionalized dipodal *bis* Schiff base chromogenic and fluorogenic chemosensors for selective and sensitive detection of Al^{3+} and Cr^{3+}

Rukhmani Chandra, Amit Kumar Manna, Meman Sahu, Kalyani Rout, Goutam K. Patra

PII: S0020-1693(19)31349-0
DOI: https://doi.org/10.1016/j.ica.2019.119192
Reference: ICA 119192

To appear in: *Inorganica Chimica Acta*

Received Date: 5 September 2019
Revised Date: 3 October 2019
Accepted Date: 3 October 2019

Please cite this article as: R. Chandra, A.K. Manna, M. Sahu, K. Rout, G.K. Patra, Simple salicylaldimine-functionalized dipodal *bis* Schiff base chromogenic and fluorogenic chemosensors for selective and sensitive detection of Al^{3+} and Cr^{3+}, *Inorganica Chimica Acta* (2019), doi: https://doi.org/10.1016/j.ica.2019.119192

Simple salicylaldimine-functionalized dipodal *bis* Schiff base chromogenic and fluorogenic chemosensors for selective and sensitive detection of Al^{3+} and Cr^{3+}

Rukhmani Chandra, Amit Kumar Manna, Meman Sahu, Kalyani Rout and Goutam K. Patra*
Department of Chemistry, Guru GhasidasVishwavidyalaya, Bilaspur (C.G)

Abstracts

Two salicylaldimine-functionalized dipodal *bis* Schiff base low cost fluorescent colorimetric chemosensors **L1** (bis([4-(2-hydroxy-3-methoxybenzyl-ideneamino)phenyl] ether) and **L2** (di[(4-phenylimino) 4-diethylsalicyl-aldehyde] ether) have been designed and synthesized. These sensors could simultaneously detect two biologically important metal ions (Al^{3+} and Cr^{3+}) by change in both absorption and fluorescence intensity in CH_3CN-H_2O (1/1, v/v) solvent mixture at physiological pH. The jobs plot analyses indicate the 2:2 binding stereochemistry for Al^{3+} and Cr^{3+} ions with both the probes **L1** and **L2**, which were further been confirmed by ^{1}H-NMR and ESI-MS studies. The binding constant values for **L1** were found to be 2.35×10^5 M^{-1} for Al^{3+} and 1.26×10^5 M^{-1} for Cr^{3+} and in case of **L2** these values are $1.46 \times 10^5 M^{-1}$ for Al^{3+} and 3.0×10^5 M^{-1} for Cr^{3+}. The detections limits of the sensor **L1**, for Al^{3+} (1.73×10^{-7}M) and Cr^{3+} (1.12×10^{-7}M) and of the sensor **L2**, for Al^{3+} (4.34×10^{-7}M) and Cr^{3+} (7.73×10^{-7}M) are far below than the limit set by the World Health Organization (WHO) for drinking water. Moreover, visible colorimetric test kitsand real samples for rapid detection of Al^{3+} and Cr^{3+} could be successively applied for all practical purposes, indicating their potential use in environmental samples.

Keywords: Salicylaldimine-functionalized *bis* Schiff base; dipodal ligands; fluorescent sensor; colorimetric sensor; cation sensing; Al^{3+} and Cr^{3+} sensors.

Corresponding Author: Tel.: 91 7587312992, *E-mail*: patra29in@yahoo.co.in

1. Introduction

The development of sensitive and selective chemosensors, which is capable of recognition of various important heavy and transition metal ions simultaneously, is an active area of current research for analytical as well as environmental and biological problem [1-4]. Among the various types of sensors, fluorescent chemosensors for metal ions have attracted much attention due to their convenient use and high sensitivity [5-7]. Furthermore, colorimetric methods are also extremely attractive because they allow naked-eye detection of color change without any use of a spectroscopic instrument [8-10]. Trivalent cations have important biological properties and are directly involved in the cell function where there is a critical control of M^{3+} (trivalent metal ion) levels [11,12]. Aluminum is the third most abundant and prevalent element (8.3% by weight) after oxygen and silicon in the earth's crust. It has been widely used in many fields, such as water treatment, food additives, medicines, production of light alloys, electronic and electrical components of different implements, building materials, various packing items etc. [13-15]. According to the World Health Organization (WHO) report, the average daily human intake of aluminum is approximately 3-10 mg. However, the unregulated amount of aluminum in human body leads to malfunction of the central nervous system, Parkinson's disease, Alzheimer's disease and amyotrophic lateral sclerosis [16-18].

Chromium, one of the most common elements in the earth's crust and seawater, exists as metallic Cr^0, Cr^{3+}, and Cr^{6+} forms. Cr^{3+} is an essential component in human nutrition whereas the Cr^{6+} is highly toxic. Cr^{3+} plays important role in metabolism of carbohydrates, fats proteins and nucleic acids by activating certain enzymes and stabilizing proteins and nucleic acids [19,20]. Further, the deficiency of Cr^{3+} in the human body often causes different health disorders including cardiovascular diseases and diabetes. However, a high concentration of chromium is very harmful to human health and can also have a negative impact on cellular structures and normal enzymatic activities [21-22]. The environmental protection agency (EPA) has set the maximum permissible level of total chromium as 0.1 mg/mL [23-25].

Due to its paramagnetic nature Cr^{3+} is the most effective fluorescent quenchers, and the lack of a selective receptor system for Cr^{3+} [26]. In the recent past, there are very few fluorescence *turn-on* sensors for Cr^{3+} have been reported [27, 28]. In contrast, Al^{3+} is diamagnetic, whose binding with receptor often enhance the fluorescence. Due to its poor coordination ability and lack

of spectroscopy characteristics, only a few Al^{3+} sensors are available in the literature as compared to transition metal ions [29-30].

As a result of the potential impact of Al^{3+} and Cr^{3+}on the environment and human health, it is essential to the development of highly selective and sensitive fluorescent chemosensors, which are capable of recognizing these metal ions by color and fluorescence responses. The most commonly employed method used for detection of theses metal ions are atomic absorption and atomic emission spectrometry, inductively coupled plasma mass spectrometry and electrochemical methods [31-34] but most of these methods require sophisticated instruments and time consuming for sample preparation protocols etc. On the contrary, fluorescence chemosensors are the best choices, due to their high sensitivity, fast response, and inexpensive technique.

Schiff bases with *o*-substituted aromatic rings have found to be most responsive for chelation with a wide range of metal ions. The coordination of metal ions through the >C=N linkage would develop intramolecular charge transfer (ICT) transition or make ligand to metal charge transfer (LMCT) transition, which could be useful for the visual sensing of the metal ions [35]. In this regard and in continuation with our earlier research work [36, 37], we report here two chemosensors bis([4-(2-hydroxy-3-methoxybenzyl-ideneamino)phenyl] ether) (**L1**) and (di[(4-phenylimino) 4-diethylsalicyl-aldehyde] ether) (**L2**) which are 1:2 condensation products of 4-(4-aminophenoxy) benzenamine with 2-hydroxy-3-methoxybenzaldehyde and 4-(diethylamino)-2-hydroxybenzaldehyde respectively for simultaneous detection of $Al^{3+}$and Cr^{3+} ions by naked eye color change from yellow to colorless and flouorescence enhancement in CH_3CN-H_2O (1:1, v/v) mixture. The strong selectivity and in-field application possibility of the developed sensors are verified using it in real sample analysis and paper strips. In addition, the theoretical calculation supported the experimental spectroscopic data for the sensing mechanism.

2. Experimental

2.1. General Information

All of the materials used for synthesis were obtained from Sigma Aldrich and used without further purification. The analytical grade solvents wereused for the overall experiments and freshly prepared double deionized water was used for dilution purpose and preparing CH_3CN-H_2O (1/1, v/v) solvent mixture. ^{1}HNMR spectra were recorded on a Bruker DRX spectrometer operating at 400 MHz in $CDCl_3$ and chemical shifts were recorded in ppm relative to TMS. UV–Visible spectra were recorded on a Shimadzu UV 1800 spectophotometer using 10 mm path length quartz

cuvettes with the wavelength in the range of 200–800 nm. The emission spectra were recorded on a Perkin Elmer LS-55 Fluorescence Spectrometer. Mass spectra were recorded on a Waters mass spectrometer using mixed solvent methanol and triple distilled water which was equipped with an ESI source. The pH measurements carried out using a digital pH meter (Merck). All the chemicals and metal salts were purchased from Merck. All the anions are of sodium salts and re-crystallized from water (Millipore) before use. Both the receptors **L1** and **L2** (1×10^{-5}M) and metal ions (1×10^{-4}M) solutions were prepared in CH_3CN-H_2O (1/1, v/v) and H_2O respectively.

2.2. X-ray data collection and structural determination

X-ray single crystal data were collected using MoKα (λ = 0.7107 Å) radiation on a BRUKER APEX II diffractometer equipped with CCD area detector. Data collection, data reduction, structure solution/refinement were carried out using the software package of SMART APEX [38]. The structures were solved by direct methods (*SHELXS-97*) and standard Fourier techniques, and refined on *F2* using full matrix least squares procedures (*SHELXL-97*) using the *SHELX-97* package [39] incorporated in *WinGX* [40]. In most of the cases, non-hydrogen atoms were treated anisotropically. Hydrogen atoms were fixed geometrically at their calculated positions following riding atom model. The crystallographic data of **L1** has been listed in Table 1. Structural information of **L1** has been deposited at the Cambridge Crystallographic Data Center (CCDC number 1893984).

Table 1. Crystallographic data and refinement parameter of the probe **L1**

Empirical formula	$C_{28}H_{24}N_2O_5$
Formula weight	468.49
Temperature/K	102.91
Crystal system	monoclinic
Space group	C2/c
a/Å	15.3630(12)
b/Å	7.5405(6)
c/Å	19.6174(15)
α/°	90
β/°	91.634(3)
γ/°	90

Volume/Å^3	2271.6(3)
Z	4
ρ_{calc}g/cm^3	1.370
μ/mm^{-1}	0.095
F(000)	984.0
Crystal size/mm^3	0.19 × 0.17 × 0.16
Radiation	MoKα (λ = 0.71073)
2Θ range for data collection/°	5.306 to 64.54
Index ranges	-22 ≤ h ≤ 19, -9 ≤ k ≤ 11, -28 ≤ l ≤ 25
Reflections collected	15672
Independent reflections	3896 [R_{int} = 0.0819, R_{sigma} = 0.0724]
Data/restraints/parameters	3896/0/161
Goodness-of-fit on F^2	1.043
Final R indexes [I>=2σ (I)]	R_1 = 0.0636, wR_2 = 0.1709
Final R indexes [all data]	R_1 = 0.0914, wR_2 = 0.2018
Largest diff. peak/hole / e Å^{-3}	0.38/-0.31

*2.3. Synthesis of **L1***

To a 30 mL dehydrated methanol solution of 4-(4-aminophenoxy)benzenamine (0.20 g, 1 mmol), 2-hydroxy-3-methoxy benzaldehyde (0.304 g, 2 mmol, in 10 mL dehydrated methanol) was added. The mixture was refluxed for 6 h at 40^{o}C, maintaining dry conditions. A light yellow precipitate was obtained. It was filtered off and washed several times with *n*-hexane and then finally recrystallized from methanol and dried in air. The solid compound was obtained with 0.374 g (80%) yield; m.p.115^{0}C.^{1}H NMR: (400 MHz, $CDCl_3$, δ ppm, TMS): 13.61 (s, 2H, -OH); 8.56(s, 2H, -CH=N); 7.20 (t, 4H, -Ar H); 7.02 (d, 4H, -Ar H); 6.94 (m, 4H, -Ar H); 6.81 (t, 2H, --Ar H) and 3.87 (s, 6H, -OCH_3) (Fig. S1). ^{13}C NMR (200 MHz, $CDCl_3$, δ ppm, TMS): *δ* 161.74, 156.12, 151.17, 148.38, 143.59, 123.62, 122.57, 119.62, 119.04, 118.54, 114.52, 56.11 (Fig. S2). ESI-MS: m/z 468.36 (M^+) (Fig. S3). FTIR/cm^{-1} (KBr): 3516(s), 2982 (w), 2870 (m), 1621(vs), 1600 (vs), 1510(vs), 1500(vs), 1435(s), 1386(m), 1182(m), 1028 (vs), 971(m), 746 (s), 613 (s) (Fig. S4). Anal. calcd. for, $C_{28}H_{24}N_2O_5$: C, 71.71 (71.78%); H, 5.14 (5.16%); N, 6.13 (5.98%).

*2.4. Synthesis of **L2***

To a dehydrated methanol solution of 4-(4-aminophenoxy)benzenamine (0.20 g, 1 mmol, 50 mL), 4-(diethylamino)-2-hydroxybenzaldehyde (0.386 g, 2 mmol, in 10 mL dehydrated methanol) was added. The mixture was refluxed for 6 h at 45^{o}C, maintaining dry conditions. A light yellow precipitate was obtained. The solid compound was obtained with 0.412 g (75%) yield.; m.p. 150^{0}C.^{1}H NMR: (400 MHz, $CDCl_3$, δ ppm, TMS): 13.62 (s, 2H, -OH) 8.41 (s, 2H, -CH=N); 7.22 (m, 4H, -Ar H); 7.16 (m, 4H, -Ar H); 7.03 (m, 4H, -Ar H); 6.25 (d, 2H, -Ar H); 6.19 (s, 2H, -OH); 3.41 (q, 8H, $-CH_2$) and 1.22 (m, 12H, $-CH_3$) (Fig. S5). ^{13}C NMR (200 MHz , $CDCl_3$, δ ppm, TMS): *δ* 163.86, 159.90, 155.18, 151.62, 144.38, 133.59, 121.95, 119.47, 109.01, 103.64, 97.70, 44.57 and 12.67 (Fig. S6). ESI-MS: m/z 551.21 (MH^+, 65%) (Fig. S7). FTIR/cm^{-1} (KBr): 3434 (m, γ-OH), 2970 (s), 2687(w, br) 1708 (s), 1632 (vs, C=N), 1493(s), 1354(vs), 1242(s), 1190, 1132(s), 839(s), 786(s) 530(s) (Fig. S8). Anal. calcd. For $C_{34}H_{38}N_4O_3$: C, 74.29 (74.15%); H, 6.91 (6.96%); N, 10.13 (10.17%).

2.5. UV-Vis titrations

L1 (4.70 mg, 0.01 mmol) and **L2** (5.52 mg, 0.01 mmol) were dissolved in 10 mL of mixed solvent CH_3CN-H_2O (1/1, v/v) individually to make a solution of 1 × 10^{-3} M and 30 µL of this solution was diluted with 2.97 mL of solvent mixture to make the final concentration of 10 µM. $Al(NO_3)_3$(3.75 mg, 0.01 mmol) was dissolved in triple distilled water (10 mL) and 1.5 - 90 µL of this Al^{3+} (1 mM) was transferred to each receptor solution **L1** and **L2** (10 µM). After mixing them for a few seconds, UV-Vis spectra were obtained at room temperature.

2.6. Fluorescence titrations

L1 (4.70 mg, 0.01 mmol) and **L2** (5.52 mg, 0.01 mmol) were dissolved in 10 mL of mixed solvent CH_3CN-H_2O (1/1, v/v) individually to make a solution of 1×10^{-3} M and 30 µL of this solution was diluted with 2.97 mL of solvent mixture to make the final concentration of 10 µM. $Al(NO_3)_3$(3.75 mg, 0.01 mmol) was dissolved in triple distilled water (10 mL) and 1.5 - 90 µL of this Al^{3+} (1 mM) was transferred to each receptor solution **L1** and **L2** (10 µM). After mixing them for a few seconds, fluorescence spectra were obtained at room temperature.

The same procedure was followed for Cr^{3+} using the solvent mixture CH_3CN-H_2O (1/1, v/v).

2.7. Job plot measurements

For Al^{3+}, **L1** (4.70 mg, 0.01 mmol) and **L2** (5.52 mg, 0.01 mmol) were dissolved in methanol (10 mL) separately. 100, 90, 80, 70, 60, 50, 40, 30, 20, 10 and 0 µL of the each receptor

L1 and **L2** solution were taken individually and transferred to vials. Each vial was diluted with 2.9 mL of mixed solvent. $Al(NO_3)_3$ (0.01 mmol) was dissolved in triple-distilled water (10 mL). 0, 10, 20, 40, 50, 60, 70, 80, 90 and 100 μL of the Al^{3+} solution were added to each diluted **L1** and **L2** solution. Each vial had a total volume of 3 mL. After shaking them for a minute, fluorescence spectra were obtained at room temperature.

The same procedure were followed for Cr^{3+} using CH_3CN-H_2O (1/1, v/v).

2.8. Competition with other metal ions

For Al^{3+}, **L** {**L1** (4.66 mg, 0.01 mmol) and **L2** (5.52 mg, 0.01 mmol)} were dissolved in the afore-mentioned CH_3CN-H_2O (1/1, v/v) solvent mixture individually (10 m**L**) and 30 μ**L** of it was diluted to 3 m**L** with the solvent mixture to make a final concentration of 10 μM. $Al(NO_3)_3$ (0.01 mmol) and $M(NO_3)_x$ (0.1 mmol) were dissolved in 10 m**L** of triple-distilled water. 30 μ**L** of each metal solution (10 mM) was taken and added to 3 m**L** of the solution of receptor **L** individually (10 μM) to give 10 equiv. of metal ions. Then, 30 μ**L** of Al^{3+} solution (10 μM) was added to the mixed solution of each metal ion and **L** to make 10 equiv. After mixing them for a few seconds, fluorescence spectra were obtained at room temperature.

The same procedure was followed for Cr^{3+} using the solvent mixture CH_3CN-H_2O (1/1, v/v).

2.9. pH effect test

A series of buffers with pH values ranging from 2 to 11 was prepared using 100 mM HEPES buffer. After a solution with the desired pH was achieved, receptor **L** {**L1** (4.66 mg, 0.01 mmol) and **L2** (5.52 mg, 0.01 mmol)} were dissolved in methanol (10 mL) individually, and then 30 μL of this solution (1 mM) was diluted to 3 mL with the above-mentioned buffers to make the final concentration of 10 μM. $Al(NO_3)_3.9H_2O$ (37.5 mg, 0.1 mmol) was dissolved in HEPES buffer (10 mL, pH 7.00). 30 μL of the Al^{3+} solution (10 mM) was transferred to each receptor solution (10 μM) prepared above. After mixing them for a few seconds, UV-Vis spectra were obtained at room temperature.

The same procedure was followed for Cr^{3+} using the solvent mixture CH_3CN-H_2O (1/1, v/v).

2.10. Binding constants using spectroscopic titration data

The binding constants for the formation of the respective complexes were evaluated using the Benesi-Hildebrand plot (eqn1).

$$1 / (A - A_o) = 1 / \{K (A_{max} - A_o)C^n\} + 1 / (A_{max} - A_o) \quad (1)$$

Ao is the absorbance of **L** at the absorbance maximum Al^{3+} (317 nm) and Cr^{3+} (313) nm for **L1** and Al^{3+} (357 nm) and Cr^{3+} (373) nm for **L2**, A is the observed absorbance at that particular wavelength in the presence of a certain concentration of the metal ion (C), A_{max} is the maximum absorbance value that was obtained at λ = 317 nm (**L1**) and 357 nm (**L2**) for Al^{3+} and λ = 313 nm (**L1**) and 373 nm (**L2**) for Cr^{3+} during titration with varying metal ion concentration, K is the binding constant (M^{-1}), which was determined from the slope of the linear plot, and C is the concentration of the concentration of the Al^{3+} and Cr^{3+} ion added during titration studies and n is the number of metal bound per ligand.

2.11. Detection limit for Al^{3+} and Cr^{3+}

Thedetectionlimit was calculated based on the UV-Vis titration for Al^{3+} and Cr^{3+}. The absorbance spectrum of **L** was measured and the standard deviation of the blank measurement was achieved. To obtain the slope, the UV-Vis absorbance at 317 nm (**L1**) and 313 nm (**L2**) for Al^{3+} and 350 nm (**L1**) and 373 nm (**L2**) for $Cr^{3+}$was plotted as a function of the corresponding metal ion concentration. The detection limit was calculated with the following equation.

Detection limit = 3σ / K

Where σ is the standard deviation of the blank measurement and K is the slope between the ratio of the UV-Vis absorbance versus metal ion concentration.

2.12. Colorimetric test kit

1 mM solution of **L** {**L1** (4.66 mg, 0.01 mmol) and **L2** (5.52 mg, 0.01 mmol)} were prepared in 10 mL CH_3CN-H_2O (1/1, v/v). Test kits were obtained by immersing filter-papers into this 1 mM solution and then dried in air to get rid of the solvent. Nitate salts of Na^+, K^+, Mg^{2+}, Ba^{2+}, Fe^{3+}, Co^{2+}, Ni^{2+}, Cu^{2+}, Zn^{2+}, Cd^{2+}, Ca^{2+}, Cr^{3+}, Hg^{2+}, Pb^{2+}, Al^{3+} were dissolved in water (10 mL) to prepare 0.1 mM solution. The above test kits were dipped into the aqueous solution of different cations solutions and then dried at room temperature to observe the color change.

2.13. Theoretical calculation methods

The GAUSSIAN-09 Revision C.01 program package was used for all calculations [41]. The gas phase geometries of the compound was fully optimized without any symmetry restrictions in singlet ground state with the gradient-corrected DFT level coupled with the hybrid exchange-correlation functional that uses Coulomb-attenuating method B3LYP [42]. Basis set 6-31++G was found to be suitable for the whole molecule.

3. Results and discussion

*3.1. Synthesis of **L1** and **L2***

The flexible Schiff-base receptors **L1** and **L2** were synthesized in single step in more than 75% yield as yellow crystalline solids via condensation reaction of 4-(4-aminophenoxy)benzenamine with 2-hydroxy-3-methoxybenzaldehyde and 4-(diethylamino)-2-hydroxy benzaldehyde respectively (Scheme 1) following reported procedures [43, 44].

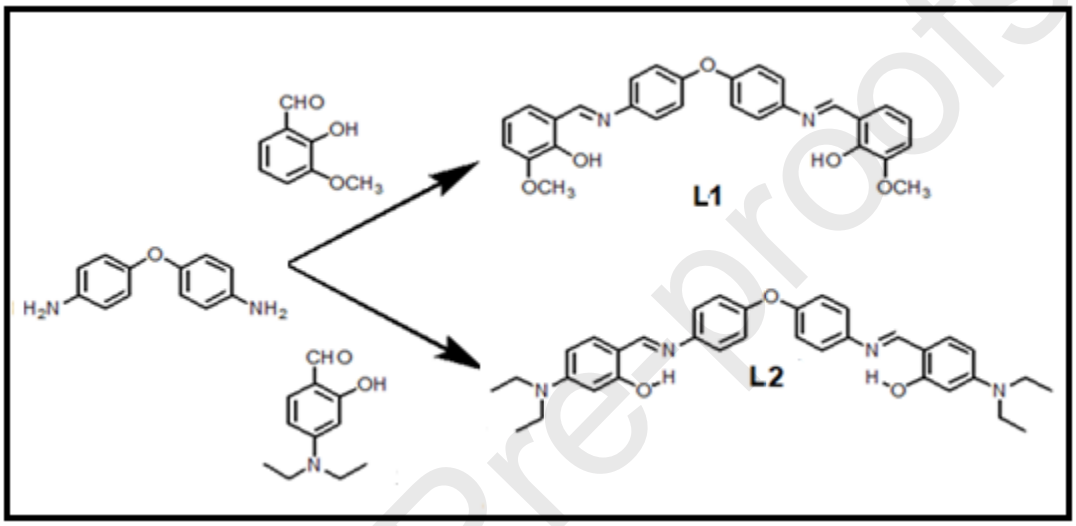

Scheme 1. Synthetic procedures of the receptors **L1** and **L2**.

DFT calculations were performed on the molecule **L1** and **L2**. The geometry optimizations staring from Gauss-view structures of **L1** and **L2** lead to global minimum as stationary level. The geometry optimized structures of the receptors **L1** and **L2** have been shown in Fig. 1 and representation of the energy of MOs and contours of selected HOMO and LUMO orbitals of the receptors have been shown in Figs. S9 and S10. The HOMO to LUMO energy gapsfor **L1** and **L2** are 7.4068 eV and 5.566 eV respectively.

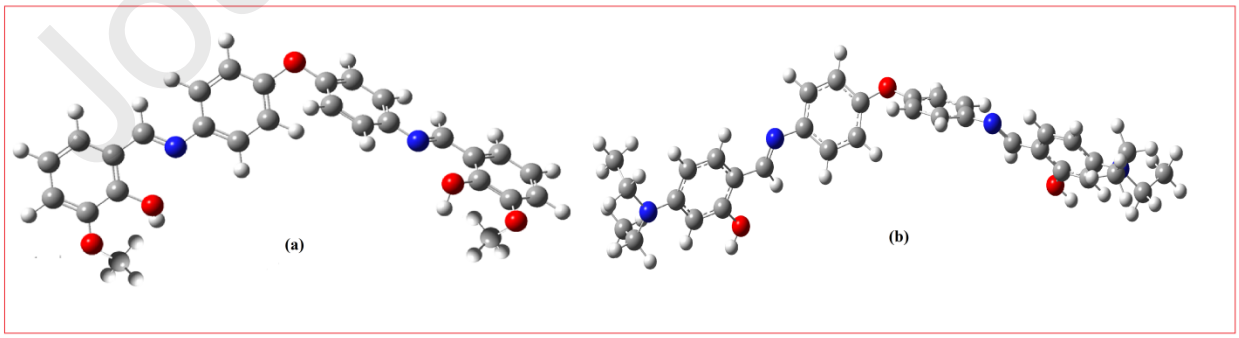

Fig.1. DFT optimized structures of molecules (a) **L1** and (b) **L2**.

The single crystals of the probe **L1** (*Bis[4-(2-hydroxy-3-methoxybenzylideneamino)phenyl] ether)* were grown by slow evaporation of the methanol solution at room temperature. **L1** was crystallized as monoclinic C2/c space group. The molecule of **L1** lies on a two-fold rotation axis, and each half exhibits an imine E configuration and an O—H···N hydrogen bond (Fig.2). The dihedral angle between the two benzene rings attached to the central O atom is 69°, and that between each of these rings and the other benzene ring in the same half of the molecule is about 24°, which makes the molecule flexible. Recently Kaabi et al. reported the single crystal structure of **L2** [45]. The two C=N bonds in **L2** were in E (trans) configuration. The dihedral angle between the two planes defined by O21 and each of the two phenyl rings is 65.00^0. However, in the crystal structure, the two halves of molecule are identical in geometry. The dihedral angles formed by COO8-O002-COO8a-C007a and COO8a-O002-COO8-C007 are 43.02^0. These angles are remarkably larger than those formed by the biphenyl-phenol rings (65.00^0). This is possibly due to the presence of two intramolecular O-H…N hydrogen–nitrogen interactions. The ligand **L2** is having a phenol–imine tautomer with eight molecules in each unit cell.The bond lengths of C-O (phenol) are 1.358 Å (2) and 1.354Å respectively, which lies in usual ranges [46].

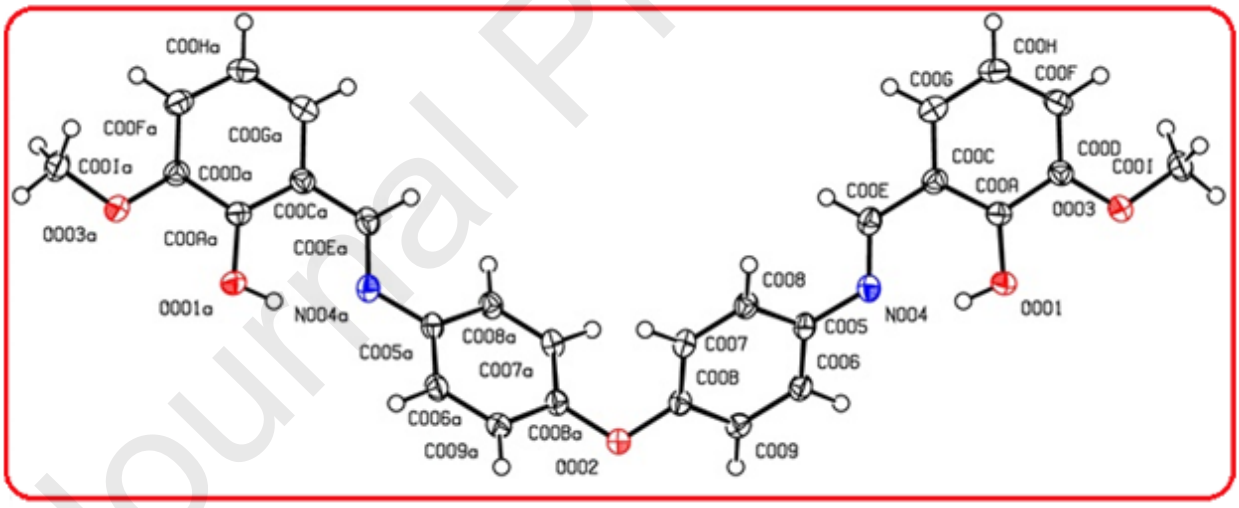

Fig.2. Crystal structure of **1**. Thermal ellipsoids are drawn at the 50% probability level.

*3.2.1. Colorimetric and spectral response of **L1** and **L2** towards various metal ions*

The colorimetric sensing ability of **L1** and **L2** towards various metal ions(Na^+, K^+, Mg^{2+}, Ba^{2+}, Fe^{3+}, Co^{2+}, Ni^{2+}, Cu^{2+}, Zn^{2+}, Cd^{2+}, Ca^{2+}, Cr^{3+}, Hg^{2+}, Pb^{2+}, Al^{3+}in CH_3CN-H_2O (1/1, v/v) was monitored by visual color change. In naked-eye experiment addition of only Al^{3+} and Cr^{3+} ions

induced a significant color change from yellow to colorless, whereas the remaining cations cause no color change at the similar condition (Fig. 3).

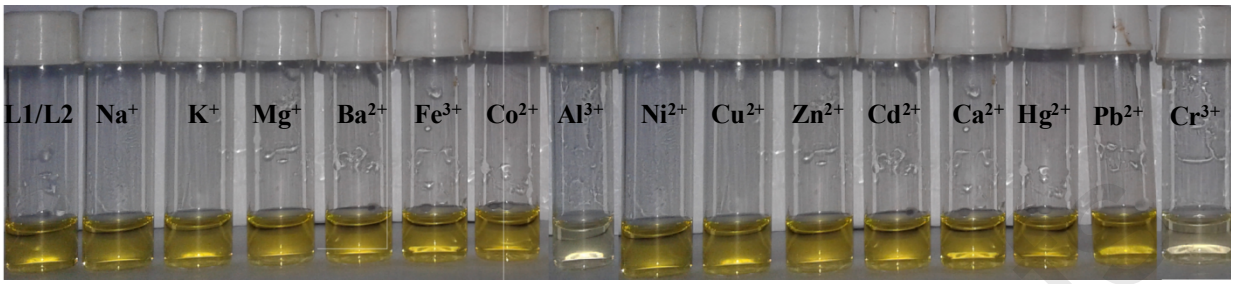

Fig.3. The color changes of **L1** and **L2** upon addition of various metal ions (3 equiv.) in CH_3CN-H_2O (1/1, v/v).

The spectroscopic properties of the receptors **L1** and **L2** towards various metal ions as Na^+, K^+, Mg^{2+}, Ba^{2+}, Mn^{2+}, Fe^{3+}, Co^{2+}, Ni^{2+}, Cu^{2+}, Zn^{2+}, Cd^{2+}, Ca^{2+}, Cr^{3+}, Hg^{2+}, Pb^{2+}, Al^{3+}were investigated in CH_3CN-H_2O (1/1, v/v) as shown in Fig.4. Here, the free receptor **L1** exhibited three absorption bands at 234, 287 and 342 nm and the receptor **L2** exhibited three bands at 271, 335 and 436 nm. Among these bands, two bands (234 and 287 nm for **L1** and 271 and 335 nm for **L2**) were assigned to π-π* transition, while the remaining bands (342 nm for **L1** and 436 nm for **L2**) were accredited to the n-π* electronic transition that originates from the promotion of non-bonding electrons of the N atom in the C=N group to an anti-bonding orbitals of receptor **L1** and **L2**. After the addition of number of different metal ions, the decrease in absorption intensity around 287 nm and 342 nm for **L1** and 436 nm for **L2** were observed only in presence of 2 equiv. of Al^{3+} and Cr^{3+}. The remaining metal ions cannot influence the absorption spectra of both the free receptor **L1** and **L2** under similar condition. Also the intensity of the absorption band at 234 nm slightly increase and small band around 335 nm of **L2** gets significant increased on addition of Al^{3+} and Cr^{3+}.

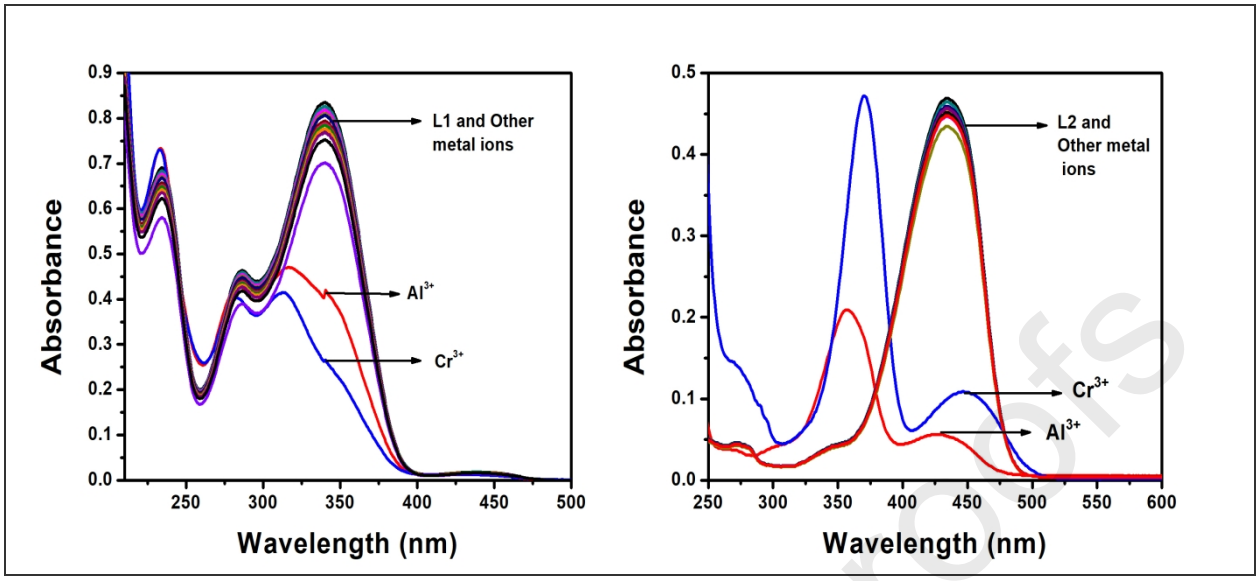

Fig.4. Absorbance spectrum of **L1** and **L2** (10μM) in CH_3CN-H_2O (1/1, v/v)in presence of different metal ions (10μM); Na^+, K^+, Mg^{2+}, Ba^{2+}, Mn^{2+}, Fe^{3+}, Co^{2+}, Ni^{2+}, Cu^{2+}, Zn^{2+}, Cd^{2+}, Ca^{2+}, Cr^{3+}, Hg^{2+}, Pb^{2+} and Al^{3+}.

Sensitivity was determined from absorption titration experiments in CH_3CN-H_2O (1/1, v/v) homogeneous mixture. In the titration experiment, upon increasing the concentration of Al^{3+} and Cr^{3+} ions (0–2 equiv.) separately, the absorbance of **L1** at 287 nm and 342 nm gets decreased and blue shifted with concomitant increase in absorbance at 234 nm, causing an well-defined isosbestic points at 272 and 230 nm for Al^{3+} and Cr^{3+} ion respectively (Fig. 5). Similarly addition of 0–2 equiv. analytes (Al^{3+} and Cr^{3+} ions) to the **L2** solution, the absorbance bands at 436 nm gradually decreased and blue shifted in each step and ultimately a new peak at 445 nm and 450 nm was appeared. Also a significant absorption band appeared simultaneously 348 nm and 373 nm with a well-defined isosbestic points at 255 and 285 nm for Al^{3+} and Cr^{3+} ions respectively (Fig. 6). Consistent with the absorption change color of the medium was changed from yellow to pale yellow in both the chemoreceptors. The metal ions (Al^{3+} and Cr^{3+}) may form tight complex with both the receptors through imine N and O site which diminish the n-π* electronic transition and intramolecular charge transfer which causes visible sensing in the ground state.

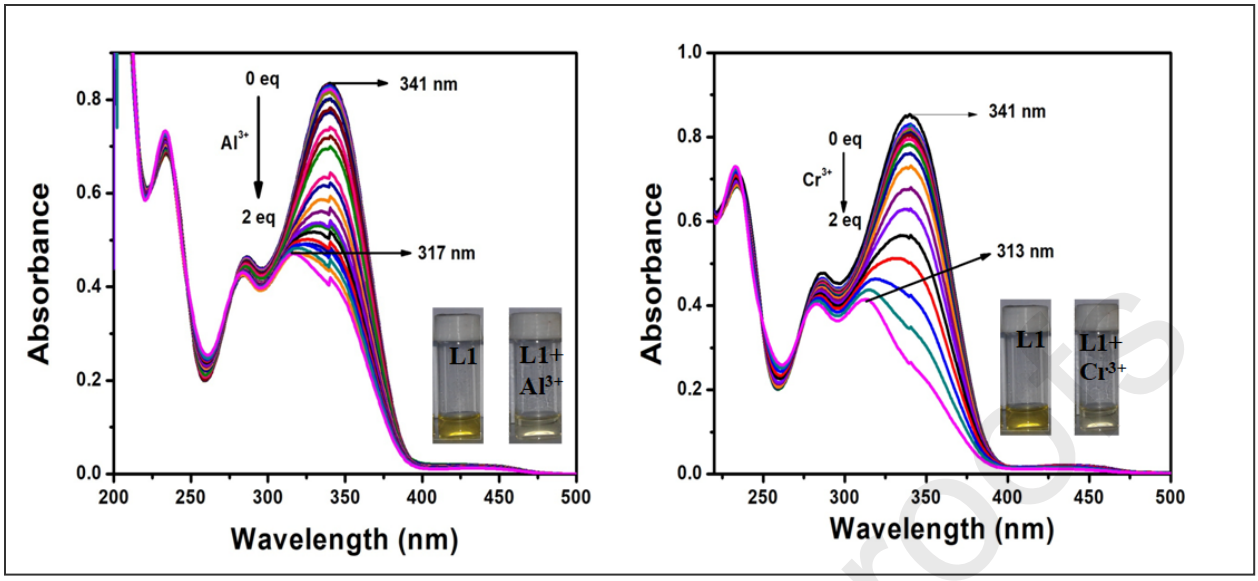

Fig.5. Absorption spectral changes of **L1** (10 μM) in the presence of different concentrations of Al^{3+} and Cr^{3+} in ranges of 0 - 2 equiv. in CH_3CN-H_2O (1/1, v/v).

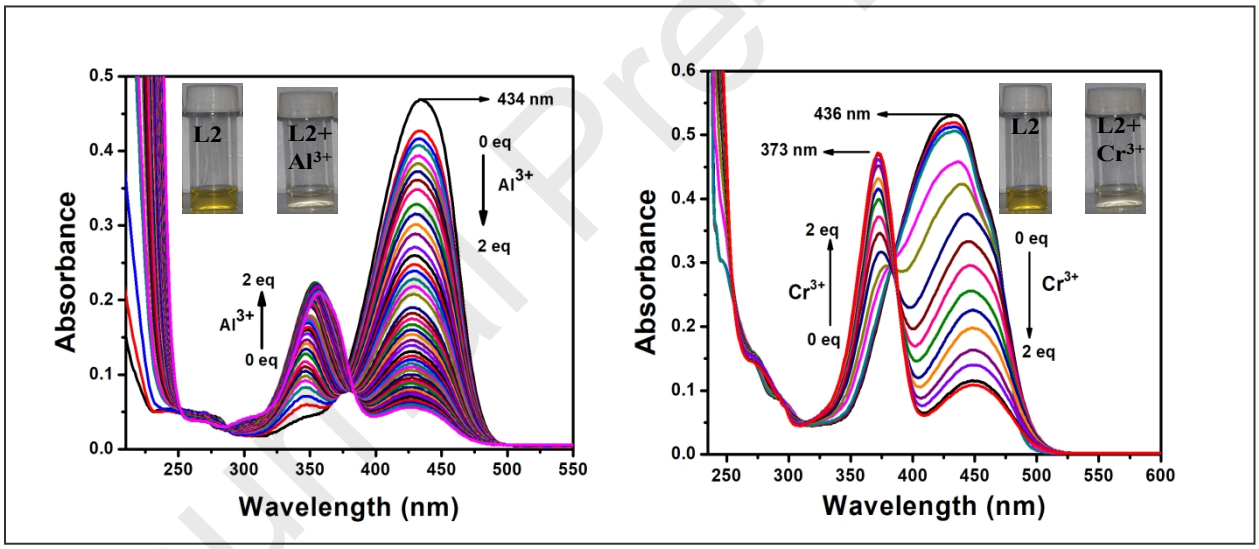

Fig.6. Absorption spectral changes of **L2** (10 μM) in the presence of different concentrations of Al^{3+} and Cr^{3+} in range of 0-2 equivalent in CH_3CN-H_2O (1/1, v/v).

The binding ability depends on size, charge and electron configuration of the metal ion and ligandin addition, the acidic nature of Al^{3+} is more compared to Cr^{3+}. So, more electron accepting nature of Al^{3+} has greater affinity to form metal complex. The experimental data showed that the absorption intensities of receptors **L1** and **L2** after addition of Al^{3+} at 317 and 423 nm fits linearly with Al^{3+} concentration, having a good R^2 value of 0.99756 and 0.99454 respectively. Similarly, absorption bands at 313 and 448 nm showed linear response with Cr^{3+} concentration with R^2 value

0.9989 and 0.98617 respectively for **L1** and **L2**. From this linear fitting, the detection limits for Al^{3+} and Cr^{3+} were determined to be 1.73 x 10^{-7}M and 1.12 x 10^{-7}M respectively for **L1** and 4.34 x 10^{-7} M and 7.73 x 10^{-7} M respectively for **L2** on the basis of 3σ/K, where σ is the standard deviation of the blank solution and K is the slope of the calibration curve (Fig. S11). These results suggest that the receptors **L1** and **L2** are very much sensitive toward Al^{3+} and Cr^{3+}. Importantly, the detection limit of these chemosensors are much lower than the WHO limit and suggests that **L1** and **L2** could be an effective sensor for the detection of aluminium and chromium in drinking water. Assuming 1:1 binding stoichiometry (*vide infra*) the association constants were calculated from the UV-vis titration profiles, as 2.35 × $10^5$$M^{-1}$ and 1.26 × 10^5 M^{-1} for **L1**-Al^{3+} and **L1**-Cr^{3+} whereas for **L2**-Al^{3+} and **L2**-Cr^{3+} were found to be 1.46 × $10^5$$M^{-1}$ and 3.00 × $10^5$$M^{-1}$ respectively by a Benesi-Hildebrand plot (Figs.S12 and S13).

3.2.2. Competitive metal ion titrations

To examine the selectivity of the receptors in complex background of competing species, the UV- vis absorption spectrum of receptors **L1** and **L2** in CH_3CN-H_2O (1/1, v/v) were investigated in the presence other metal ions. Upon treatment with 2 equiv. of Al^{3+} and Cr^{3+} separately in the presence of equal equiv. of commonly employed interfering species, there was no obvious interference for the detection of Al^{3+} and Cr^{3+} (Fig.7). From the competitive experiment we found that, both the metals do not interfere with each other when present in same equiv. and consistent upto 2 fold higher concentrations.

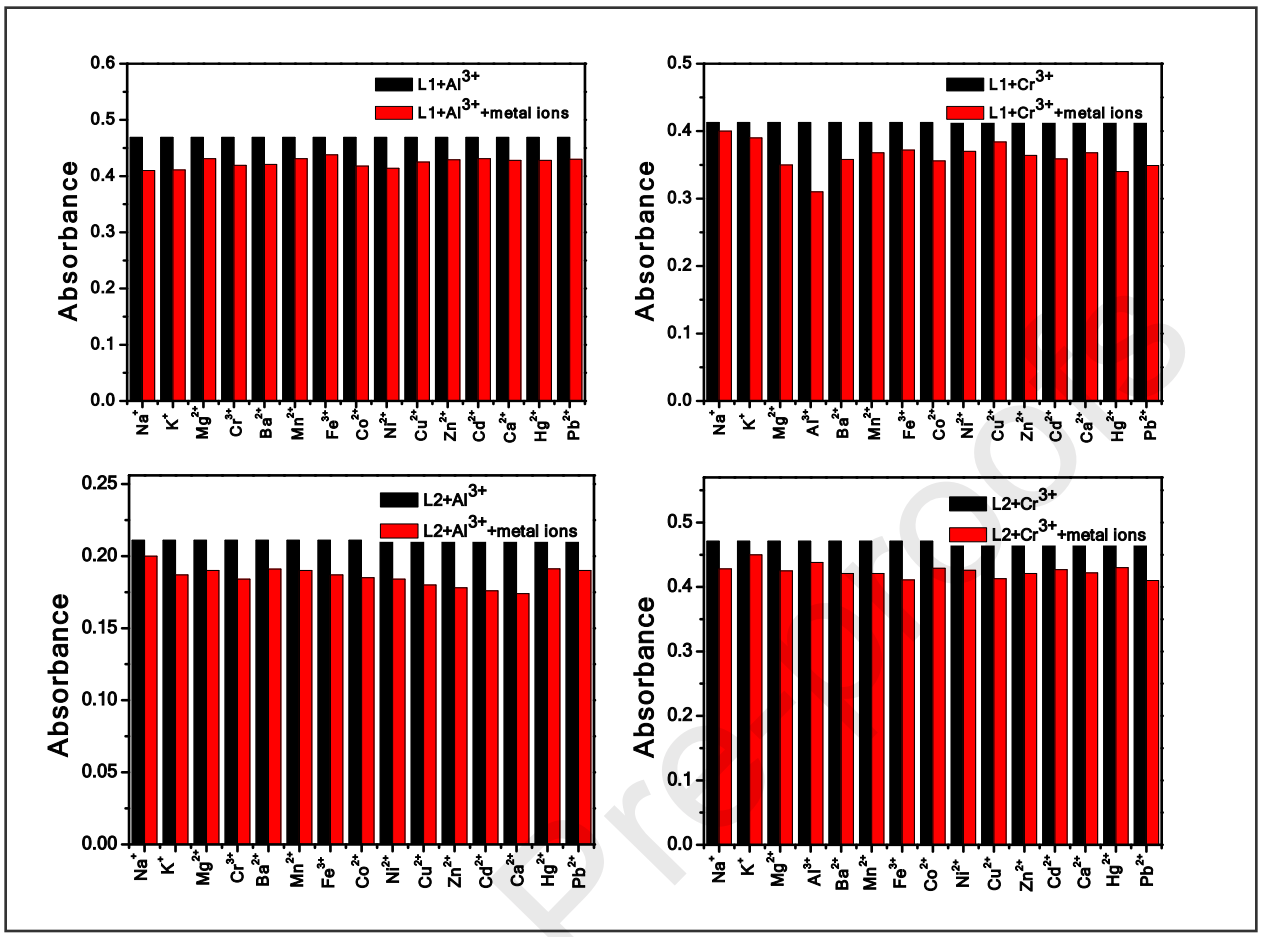

Fig.7. Selectivity of **L1** and **L2** for Al^{3+} and Cr^{3+} ions in the presence of other competitive metal ions in (10μM), the absorption wavelength were centered at 317/313 nm (**L1**) and 423/448 nm (**L2**), respectively for Al^{3+} and Cr^{3+} ions. Black bars represent absorption intensity after the addition of Al^{3+} and Cr^{3+} ions. Red bars represent the subsequent addition of the appropriate metal ion (Na^{+}, K^{+}, Mg^{2+}, Ba^{2+}, Mn^{2+}, Fe^{3+}, Co^{2+}, Ni^{2+}, Cu^{2+}, Zn^{2+}, Cd^{2+}, Ca^{2+}, Cr^{3+}, Hg^{2+}, Pb^{2+}, Al^{3+}) CH_3CN-H_2O (1/1, v/v).

*3.3. Fluorescence spectroscopic studies of **L1** and **L2** in presence of various metal ions*

We have investigated the emission studies of metal ion binding properties of receptor **L1** and **L2** towards different metal ions (20 equiv.) in CH_3CN-H_2O (1/1, v/v) (Fig.8). The free receptor **L1** showed a broad band emission spectrum with a maximum peak centered at 530 nm when excited at 350 nm. Compared to other metal ions examined, only Al^{3+} and Cr^{3+}can cause the blue shift of the emission maxima of **L1** from 530 to 480 nm (in case of Al^{3+}) and 530 to 508 nm (in case of Cr^{3+}). Titration experiments were also performed with separately additions of Al^{3+} and Cr^{3+} (0-20 equiv.) to the CH_3CN-H_2O (1/1, v/v) solution of **L1**. In both the cases, a considerable

decrease in the main emission peak at 530 nm and upon further additions of Al^{3+} and Cr^{3+} ions, a new peak generated with a hypsochromic shift (blue shift) centered at 480 nm (for Al^{3+}) and 508 nm (for Cr^{3+}) and reached saturation when 20 equiv. of Al^{3+} and Cr^{3+} ions were separately added. Further increasing of Al^{3+} and Cr^{3+} did not cause significant fluorescence emission changes (Fig.9). The blue shift in the fluorescence spectra were due to the change of the ICT properties of the interacted species between the metal ions and the donor atom of the receptor **L1**.

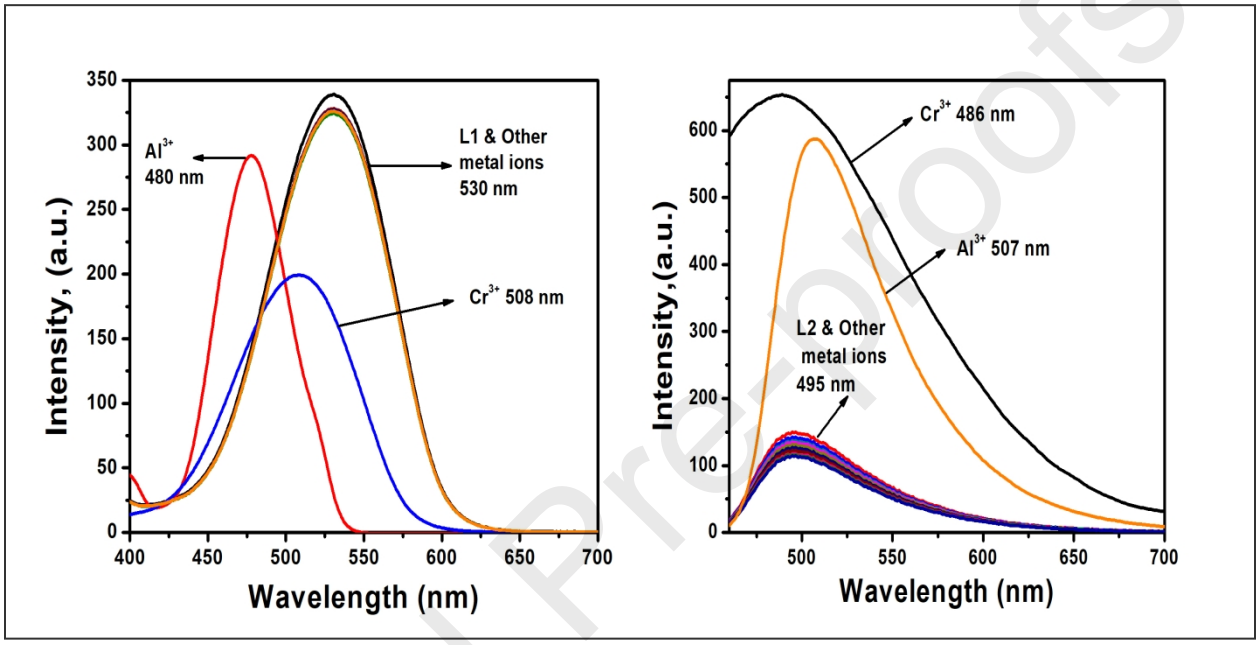

Fig.8. Fluorescence spectrum of **L1** (excited wavelength 350 nm) and **L2** (excited wavelength 430 nm) 10µM in CH_3CN-H_2O (1/1, v/v) solution in presence of different metal ions (10µM) such as Na^+, K^+, Mg^{2+}, Ba^{2+}, Mn^{2+}, Fe^{3+}, Co^{2+}, Ni^{2+}, Cu^{2+}, Zn^{2+}, Cd^{2+}, Ca^{2+}, Cr^{3+}, Hg^{2+}, Pb^{2+}, Al^{3+}.

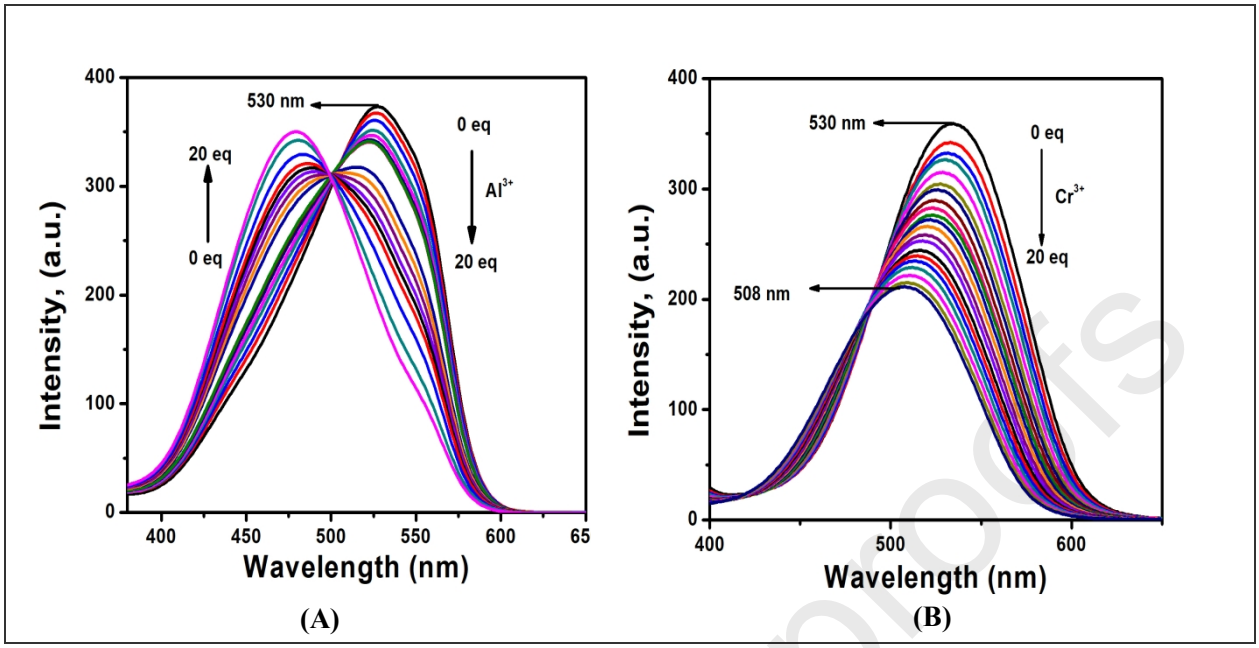

Fig.9. Changes in fluorescence spectra of solution **L1** (10μM) upon incremental addition Al^{3+} and Cr^{3+} in CH_3CN-H_2O (1/1, v/v).

In the absence of Al^{3+} and Cr^{3+}, **L2** (10 μM) is characterized by very weak emission band centered at 490 nm (on excitation at 430 nm) due to the excited state intramolecular proton transfer (ESIPT) from phenolic –OH to azomethaine-N and rotation across the C=N bond (*cis/trans* isomerization) [47]. The weak fluorescent nature of **L2** may be a consequence of strong inter and intramolecular hydrogen bonding which may be prevent the availability of the lone pairs over nitrogen leading to the prevent of PET and the fast inter conversion of the *cis* and *trans* forms of **L2**. Due to the presence of diethyl amine (DEA) group in the **L2**, enhanced the hydrogen binding ability which ultimately affected the availability of the lone pair on the N atom for PET and provided planarity and rigidity to **L2** and finally became responsible for its weak fluorescent nature. Upon concomitant additions of Al^{3+} and Cr^{3+} (0-20 equiv.) to the CH_3CN-H_2O (1/1, v/v) **L2** solution we obtained fully developed emission bands at 507 nm and 486 nm respectively and a stable chelation of **L2** with Al^{3+} and Cr^{3+} (Fig.10.). The enhancement in the fluorescence were assigned due to the binding of Al^{3+} and Cr^{3+} with donor atoms of **L2**, which ultimately led to prevents of ESIPT and *cis-trans* isomerization around the C=N bond. The hydroxyl group seems to play an important role in the identification of the Al^{3+} by strengthening the CHEF and hence prevents both the C=N isomerization and PET in **L2**, resulting in a strong fluorescence intensity. Furthermore, upon separate respective additions of other metal ions to the **L2**, no obvious

fluorescence enhancement could be observed, indicating that this change were specific only for Al^{3+} and Cr^{3+}. The selectivity of **L1** and **L2** for Al^{3+} and Cr^{3+} has been plotted as a bar graph in Fig.S14.

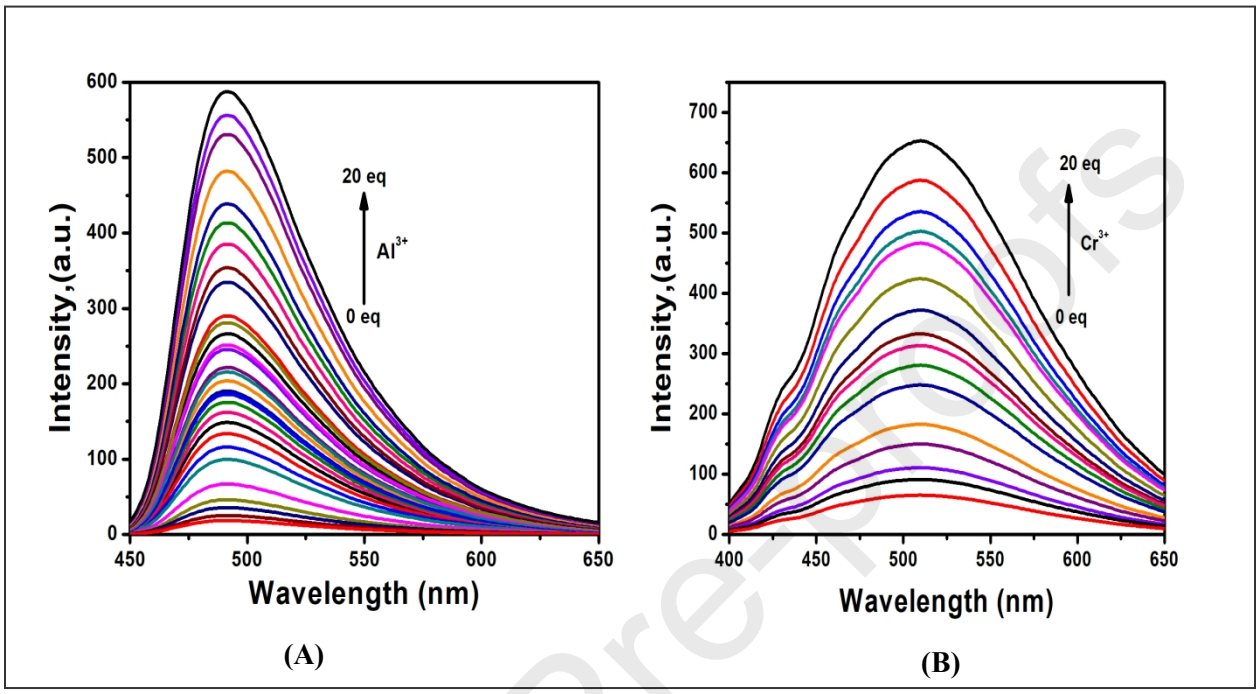

Fig.10. Changes in fluorescence spectra of solution **L2**(10μM) upon incremental addition (0-20 equiv.) of $Al^{3+}$and Cr^{3+} in CH_3CN-H_2O (1/1, v/v).

The quenching of emission intensity of **L1** in presence of Al^{3+} and Cr^{3+} ions was analyzed by Stern Volmer analysis [48] using the equation,

$$I_0/I = 1 + K_{sv}[Q]$$

Where I_0 is the emission intensity of the free receptor **L1**, I is the emission intensity of **L1** in presence of various concentration of analytes (Al^{3+} and Cr^{3+}), K_{sv} is the Stern Volmer constant and [Q] is the concentration of quencher.From the plot a linear dependency of I_0/I with analytes ($Al^{3+}$and Cr^{3+}) concentration were observed with the corresponding regression coefficient value (R^2) were 0.9871 and 0.9834 respectively, indicates the static quenching mechanism. The values of K_{sv} were calculated to 2068.88 and 2782.76 M^{-1} for Al^{3+} and Cr^{3+} respectively from the slope of these calibration curve (Fig. 11).

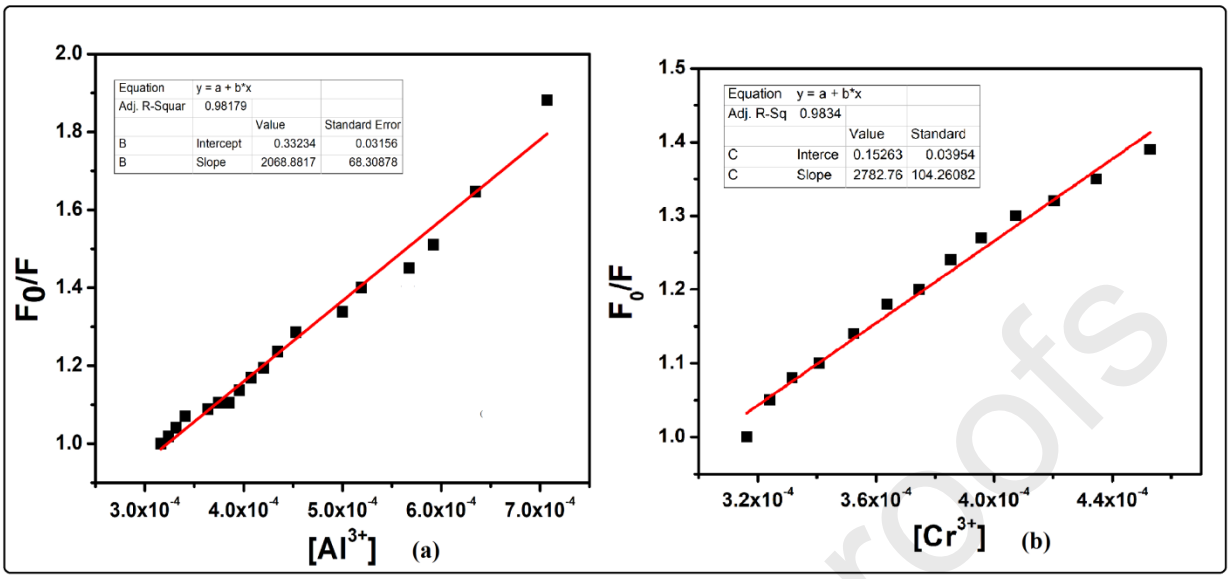

Fig.11. Stern Volmer plot of **L1** in the presence of (a) Al^{3+} and (b) Cr^{3+}.

*3.4. Stoichiometry and binding mechanism of sensing of the probes **L1** and **L2** with metal ions*

To investigate the binding characteristics of **L1** and **L2** towards Al^{3+} and Cr^{3+}, Job's titration method based on absorbance were performed, in which the absorption intensity reached to a maximum at the 0.5 molar ratio for the both metal ions, indicated that **L1** and **L2** bound to Al^{3+} and Cr^{3+} with either 1:1 or 2:2 ratio (Fig.S15). As in the *bis*-Schiff base ligands **L1** and **L2** the effective distance between two arms is very large, thus 1:1 binding not possible. Furthermore, the 2:2 binding stoichiometry were confirmed through mass spectral studies.In the positive ion mass spectrum peaks obtained at m/z =495.25 [2**L1**+2Al^{3+}] and m/z =520.25 [2**L1**+2Cr^{3+}] for **L1** and m/z =575.20 [2**L2**+2Al^{3+}], m/z =602.09[2**L2**+2Cr^{3+}] for **L2** (Fig.S16; *Z*=2 in each case) confirm 2:2 binding.

For better understanding the binding nature of **L1** and **L2** with Al^{3+}, and Cr^{3+}ions, ^{1}H-NMR spectra was recorded with and without these metal ions. Both the receptors **L1** and **L2** showed chemical shift value δ at 13.8 ppm and 13.7 ppm due to phenolic protons and 8.6 ppm and 8.4 ppm due to azomethine protons respectively. Upon binding with Al^{3+}, the phenolic protons almost disappeared because of deprotonation of phenolic groups (Fig. 12). The azomethine proton and the aromatic protons shift at higher δ values, which might be attributed to ligand to metal charge transfer. Overall changes in the chemical shifts of the protons in the **L**-Al^{3+} and **L**-Cr^{3+} adducts (where **L** = **L1** and **L2**) clearly reveals that the aldimine nitrogen (-CH=N) and -OH of **L** (both **L1** and **L2)** taking part in the complexation process. The most probable reason for this observation is

the formation of symmetrical dinuclear/dimeric complexes of two ligands with two metal ions (Scheme 2).

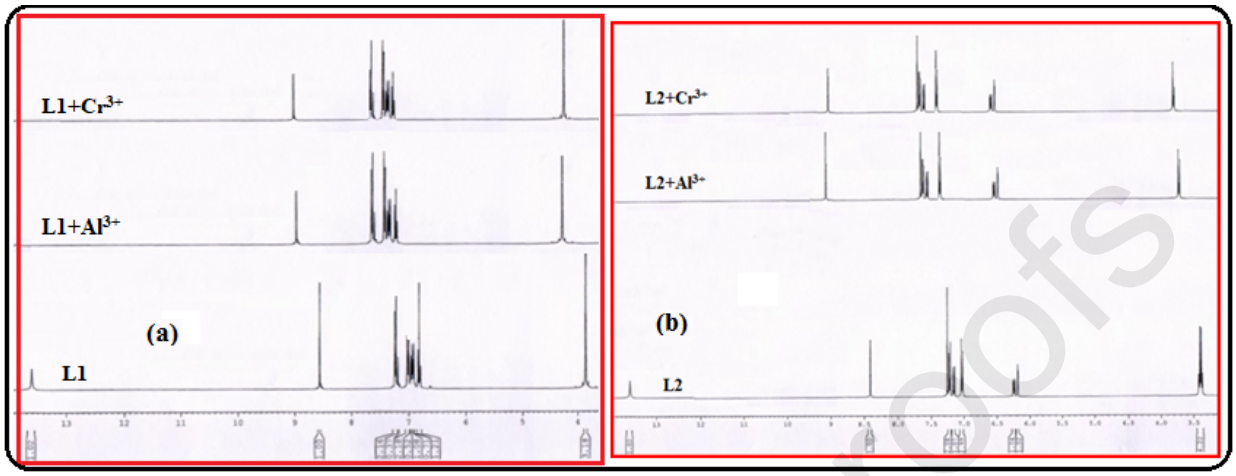

Fig.12. partial ^{1}H NMR spectra of (a) **L1, L1-** Al^{3+}, **L1-** Cr^{3+} and **(b) L2, L2-** Al^{3+}, **L2-** Cr^{3+}.

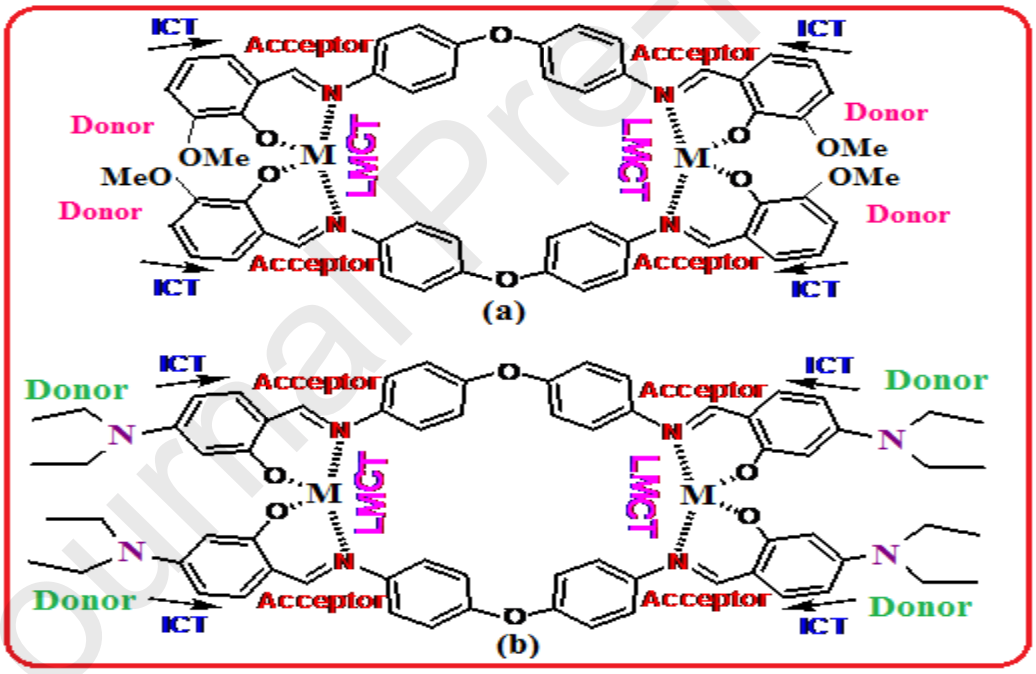

Scheme 2 Binding mechanism of **L1** and **L2** with M (M = $Al^{3+}$and Cr^{3+}).

3.5. pH effect test

It is well- known that fluorescence sensors based on the electron donor/acceptor ends are usually hindered by the concentration of protons in the medium for identifications of the metal ions. Thus, for many practical applications, it is very necessary whether the sensors are active or

not at the suitable pH conditions for successful operation. Therefore, we measured the fluorescence intensity of **L1** and **L2** and their Al^{3+} and Cr^{3+} adducts between pH 2 and 13. In acidic media with a pH range of 1-4, the fluorescence intensity of the **L1** at 530 nm beginning to quench gradually. On the other hand, the fluorescence intensity did not change over a wide pH range of 4-12 (Fig.S17A).While the free receptor **L2** are very weekly fluorescent in the pH range of 2-13. However, in the presence of 2 equiv. of Al^{3+} and Cr^{3+} separately, a significant increase in the emission intensity of **L2** recorded at 507 and 486 nm in the same pH range (4-8) were observed reaching a maximum at pH 8.0 and then decrease rapidly with a further increase in pH (Fig.S17B). The fluorescence intensity decrease in the acidic (pH <6) region due to protonation of phenolic hydroxyl group of **L2** and hence decreases the chelation ability of **L2**. Again the decreasing emission intensity in basic (pH >9) region has been explained due to ICT [47], which hampered the complexation.Hence, the emission intensity is stable over this wide range of pH (5-9) and well-suitable for applications under physiological pH conditions.

*3.6. Reversibility study of the probes **L1** and **L2***

Reversibility is a pre-requisite in developing novel sensor for practical application. Consequently, we investigated the chemical reversibility of the binding of the probes **L1** and **L2** towards Al^{3+} and Cr^{3+} by using sodium nitrate ($NaNO_3$). The absorption intensity of the **L**-M adduct (Where, **L** = **L1** and **L2** and M = Al^{3+} and Cr^{3+}) returning to original level upon addition of two equiv. of $NaNO_3$ (Fig. 13) solution along with the color of the solution changed back to the original yellow instantly, indicating the regeneration of the receptor **L1** and **L2.** Again, upon addition of Al^{3+} and Cr^{3+} ions solution, the absorption intensity of **L1** at 341 nm was blue shifted to lower wavelength at 317 and 313 nm respectively for Al^{3+} and Cr^{3+} ions but in case of **L2**, absorbance band at 436 nm was decreased and a new peak at 348 nm and 373 nm appeared respectively for Al^{3+} and Cr^{3+} ions. This ensures that **L1** and **L2** to be a sensitive sensors which can be applied in environmental analysis.

If Al^{3+} and Cr^{3+} both the ions are present in the real sample then the color of the CH_3CN-H_2O (1:1, v/v) solution of **L1** and **L2** will be yellow. Thus the detection of Cr^{3+} in presence of Al^{3+} in real sample is somewhat difficult. This problem can be solved by using the complexing agent cupferron, as it precipitated with Al^{3+} and excess addition has no role towards Cr^{3+} at that condition. Thus no problem arises for detection of Cr^{3+} from the mixture of Al^{3+} and Cr^{3+}.

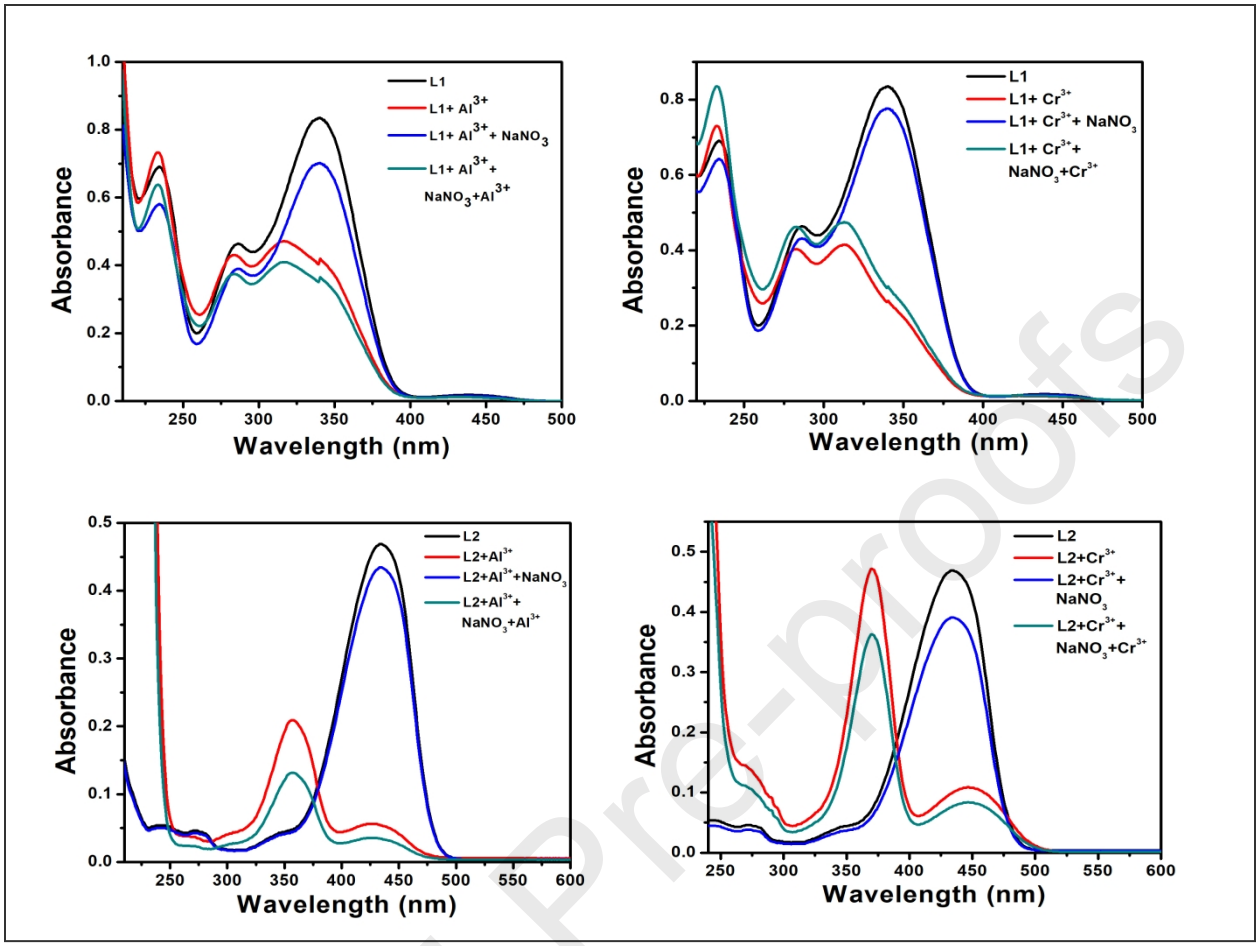

Fig.13. Reversible investigation of **L1** and **L2** (10 μM) for $Al^{3+}$and Cr^{3+}(10 μM) upon the addition of $NaNO_3$(10 μM) in CH_3CN-H_2O (1/1, v/v).

*3.7. Application of the chemosensors **L1** and **L2** in real samples*

In order to determine the environmental application of the chemosensors **L1** and **L2**, artificial Al^{3+} and Cr^{3+} contaminated sample has been prepared. The tap water samples were spiked with Al^{3+} and Cr^{3+} standard solutions at different concentration levels, and then tested their concentrations with the proposed method. The percentage of recovery along with standard deviations of the spiked samples analysed by the probe **L1** and **L2** give satisfactory results and good R.S.D. values (Tables 2 and 3).

Table 2 Determination of Al^{3+} and Cr^{3+} ions in tap water samples by the probe **L1**

Metal ion	**Spiked amount (μM)**	**Recovered amount(μM)**	**%Recovery± SD (n=3)**
Al^{3+}	10	9.42	94.2 ± 2.2
	20	19.80	99.0 ± 1.2

Cr^{3+}	10	9.23	92.3 ± 1.8
	20	20.76	103.55 ± 1.3

Table 3 Determination of Al^{3+} and Cr^{3+} ions in tap water samples by the probe **L2**

Metal ion	**Spiked amount (μM)**	**Recovered amount(μM)**	**%Recovery± SD (n=3)**
Al^{3+}	10	9.45	94.5 ± 2.1
	20	19.60	98.0 ± 1.3
Cr^{3+}	10	9.16	91.6 ± 1.4
	20	20.80	104.0 ± 1.5

3.8. Colorimetric test-kits

To check the practical application of the probes **L1** and **L2**, test kits were prepared by immersing papers in a CH_3CN solution of **L1** and **L2** and then dried in air. These test kits were used to sense Al^{3+} and Cr^{3+} ions among different cations. When the test kits coated with receptors **L1** and **L2** were added into different cation solutions, the obvious color change were observed only with Al^{3+} and Cr^{3+} in CH_3CN-H_2O (1/1, v/v) solution which have been shown in Fig.14. Hence, the test kits coated with receptors **L1** and **L2** solution would be suitable for simultaneously detection of Al^{3+} and Cr^{3+} by showing color changesin the presence of different metal ions.

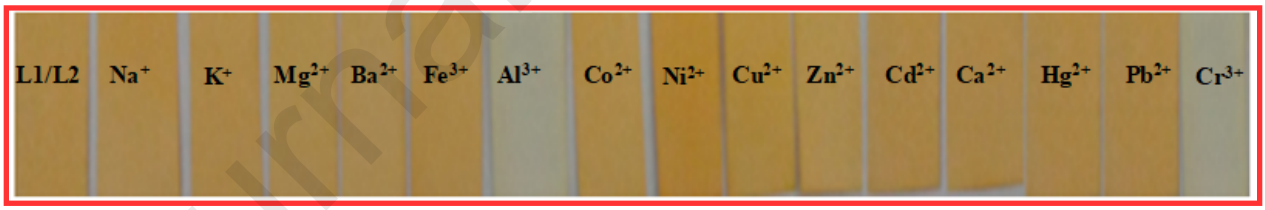

Fig.14. Photographs of the test kits with **L1** and **L2** for detecting the Al^{3+} and Cr^{3+} ions in acetonitrile-water solution (1:1, v/v) with other cations.

3.9. Comparison of L1 and L2 with other trivalent (Al^{3+} and Cr^{3+}) chemosensors

The probe **L1** and **L2**, have been compared with some other recently reported colorimetric trivalent (Al^{3+} and Cr^{3+}) chemosensors (Table 4). Our system has some advantages over the others. In our method **L1** and **L2** have been prepared by facile, single step synthetic procedure, using inexpensive reagents without troublesome and chromatographic purification. They have very

quick response time and wide linear response range. They work in $CH_3CN–H_2O$ (1 : 1, v/v). It has fairly low detection limits and high association constants.

Table 4 Comparison of **L1** and **L2** with other colorimetric trivalent chemosensors

Probe	**No. of steps involved**	**Solvent**	**LOD**	**K_a**	**Ref**
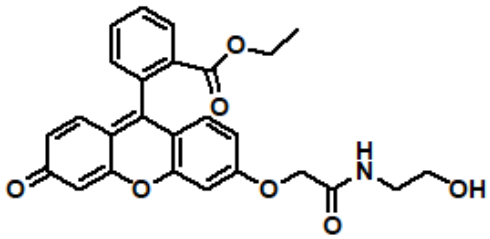	3	Pure CH_3CN	0.3μM(Al^{3+}) 0.5μM(Cr^{3+})	$6.46x10^9$ M^{-2}(Al^{3+}) $1.58x10^4$ M^{-1}(Cr^{3+})	49
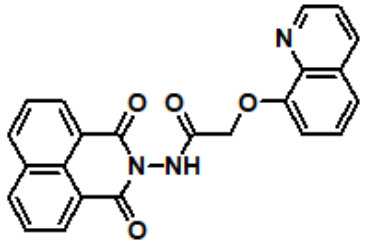	3	CH_3CN-HEPES Buffer (40/60, v/v)	23μM(Al^{3+}) 25μM(Cr^{3+})	$8.77x10^3$ M^{-1}(Al^{3+}) $5.67x10^3$ M^{-1}(Cr^{3+})	50
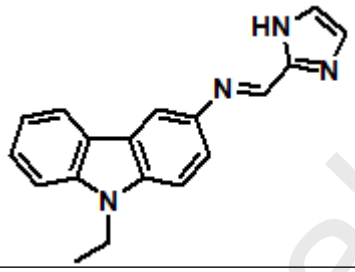	3	THF-H_2O (8:2)	0.38nM(Al^{3+}) 0.38nM(Cr^{3+})	Not determine-d	51
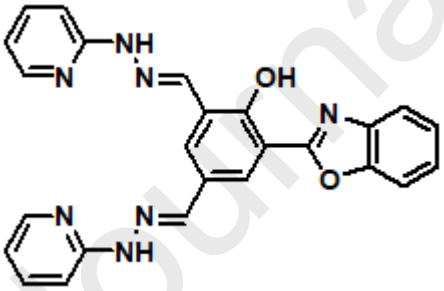	2	H_2O-EtOH (8:2)	0.5μM(Al^{3+}) 0.2μM(Cr^{3+})	$2.00x10^4$ M^{-1}(Al^{3+}) $5.50x10^4$ M^{-1}(Cr^{3+})	52
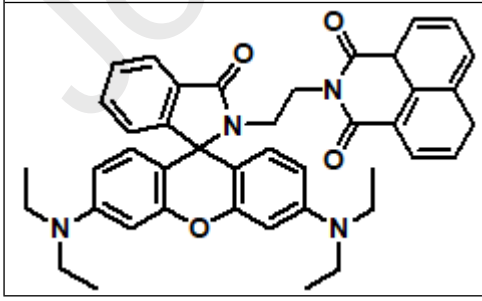	3	CH_3OH-H_2O Buffer (6/4, v/v)	1.74nM(Al^{3+}) 2.36nM(Cr^{3+})	$1.00x10^4$ M^{-1}(Al^{3+}) $2.60x10^2$ M^{-1}(Cr^{3+})	53

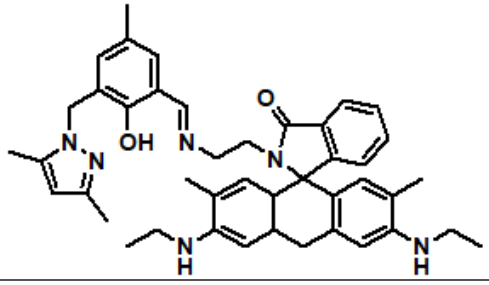	3	CH_3OH-H_2O (1/1, v/v)	0.34μM(Al^{3+}) 0.31μM(Cr^{3+})	8.20x10^4 M^{-2}(Al^{3+}) 6.00x10^4 M^{-1}(Cr^{3+})	54
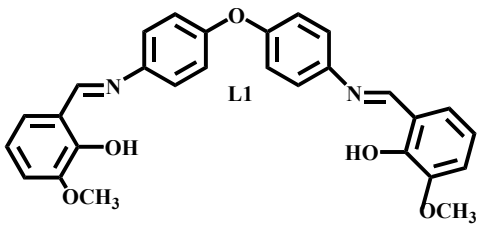	1	CH_3CN-H_2O (1/1, v/v)	0.17μM(Al^{3+}) 0.12μM(Cr^{3+})	2.35x10^5 M^{-1}(Al^{3+}) 1.26x10^5 M^{-1}(Cr^{3+})	This work
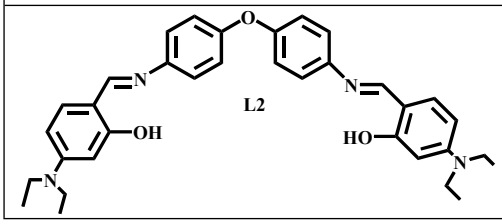	1	CH_3CN-H_2O (1/1, v/v)	0.43μM(Al^{3+}) 0.77μM(Cr^{3+})	4.34x10^5 M^{-1}(Al^{3+}) 7.73x10^5 M^{-1}(Cr^{3+})	This work

4. Conclusion

In conclusion, we report here two simple salicylaldimine-functionalized dipodal *bis* Schiff base fluorescent colorimetric chemosensors **L1** and **L2** for easy and convenient detectionof Al^{3+} and Cr^{3+}over the other competing biologicallyrelevant metal ions in CH_3CN-H_2O (1:1, v/v). These chemosensors exhibited visual color change from yellow to colorless upon addition of Al^{3+} and Cr^{3+}. The fluorescent intensity of **L1** increases upon addition of Al^{3+} and Cr^{3+} in CH_3CN-H_2O (1:1, v/v), whereas in case of **L2**, fluorescent intensity increases. The binding abilities of the probes **L1** and **L2** with Al^{3+} and Cr^{3+} were established by the combined UV-Vis, Fluorescence, ^{1}H-NMR and ESI-MS methods. The detection limits of **L1** for Al^{3+} (1.73×10^{-7}M) and Cr^{3+} (1.12×10^{-7}M) and of the sensor **L2**, for Al^{3+} (4.34×10^{-7}M) and Cr^{3+} (7.73×10^{-7}M) are far lower than those set by the WHO guidelines, thus these could be effective sensors for the detection of Al^{3+} and Cr^{3+} in drinking water. **L1** and **L2** could be successfully applied to test kits and real samples for detection of Al^{3+} and Cr^{3+}.

Acknowledgements

G.K.P would like to thank the Department of Science and Technology (SR/FST/CSI-264/2014; EMR/2017/001789) and Department of Biotechnology, Government of India, New

Delhi for financial support. A.K.M. thanks the CSIR, Government of India for financial support as a form of fellowship.

Supporting Information Summary

CCDC number 1893984contains the supplementary crystallographicdata for the probe **L1**. The data can be obtained free of charge from the Cambridge Crytallographic Data Centre, 12 Union Road, Cambridge CB21EZ, UK; Fax: (+44)1223-336-033; or email: deposit@ccdc.cam.ac.uk: Supplementary data containing Fig. S1-S17 of this article can be found online at……..

References

[1] D.P. Perl, D.C. Gajdusek, R.M. Garruto, R.T. Yanagihara, C.J. Gibbs, Intra neuronal aluminium accumulation in amyotrophic lateral sclerosis and Parkinsonism-dementia of Guam, Science 217 (1982) 1053-1055.

[2] Y.W. Liu, C.H. Chen, A.T. Wu, A turn-on and reversible fluorescence sensor forAl^{3+}ion, Analyst 137 (2012) 5201-5203.

[3] J.H. Lee, H.Y. Kim, S.J. Kim, J.Y. Noh, E.J. Song, C. Kim, J.H. Kim, Fluorescent dye containing phenol-pyridyl for selective detection of aluminum ions, Dyes Pigments 96 (2013) 590-594.

[4] D.G. Weller, A.J. Gutierrez, C. Rubio, C. Revert, A. Hardisson, Dietary intake of aluminum in a Spanish population (Canary Islands), J. Agric. Food Chem. 58 (2010) 10452-10457.

[5] (a) B. Valeur, I. Leray, Design principles of fluorescent molecular sensors for cation recognition, Coord. Chem. Rev. 205 (2000) 3-40;

(b) C. Wang, X. Yang, S. Wang, D. Schipper, R.A. Jones, Construction of a large high-nuclearity Cd−Sm schiff base cluster with nanoscale inner cavity as luminescent probe for metal cations, Cryst. Growth Des. 19 (2019) 2149-2154.

(c) C. Wang, X. Yang, S. Wang, T. Zhu, L. Bo, L. Zhang, H. Chen, D. Jiang, X. Dong and S. Huang, Anion dependent self-assembly of drum-like 30- and 32-metal Cd–Ln nanoclusters: visible and NIR luminescent sensing of metal cations, J. Mater. Chem. C 6 (2018) 865-874.

[6] K.K. Upadhyay, A. Kumar, Pyrimidine based highly sensitive fluorescent receptor for Al^{3+} showing dual signalling mechanism, Org. Biomol. Chem. 8 (2010) 4892-4897.

[7] K. Soroka, R. Vithanage, D.A. Philips, B. Walker, P.K. Dasgupta, Fluorescence properties of metal complexes of 8-hydroxyquinoline-5-sulfonic acid and chromatographic applications, Anal. Chem. 59 (1987) 629-636.

[8] O. Tavakoli, H. Yoshida, Effective recovery of harmful metal ions from squidwastes using subcritical and supercritical water treatments, Environ. Sci. Tech-nol. 39 (2005) 2357-2363.

[9] D.P. Perl, A.R. Brody, Alzheimer's disease: X-ray spectrometric evidence of aluminum accumulation in neurofibrillary tangle-bearing neurons, Science 208 (1980) 297-299.

[10] G.D. Fasman, Aluminium and Alzheimer's disease: model studies, Coord. Chem. Rev. 149 (1996) 125-165.

[11] R. Sladek, A genome-wide association study identifies novel risk loci for typediabetes, Nature 445 (2007) 881-885.

[12] X. Sun, Y.W. Wang, Y. Peng, A selective and ratiometric bifunctional fluorescent probe for Al^{3+}ion and proton, Org. Lett. 14 (2012) 3420-3423.

[13] P. Nayak, Aluminum: impacts and disease, Environ. Res. 89 (2002) 101-115.

[14] J.R. Walton, Evidence that ingested aluminum additives contained in processed foods and alum-treated drinking water are a major risk factor for Alzheimer's disease, Curr. Inorg. Chem. 2 (2012) 19-39.

[15] P.F. Good, C.W. Olanow, D.P. Perl, Neuromelanin-containing neurons of the substantianigra accumulate iron and aluminum in Parkinson's disease: a LAMMA study, Brain Res. 593 (1992) 343–346.

[16] G.D. Fasman, Aluminum and Alzheimer's disease: model studies, Coord. Chem. Rev. 49 (1996) 125-165.

[17] J.R.J. Walton, An aluminum-based rat model for Alzheimer's disease exhibits oxidative damage inhibition of PP2A activity, hyperphosphorylated tau, and granulovacuolar degeneration, Inorg. Biochem. 101 (2007) 1275-1284.

[18] J.L. Ren, J. Zhang, J.Q. Luo, X.K. Pei, Z.X. Jiang, Improved fluorimetric determination of dissolved aluminum by micelle-enhanced lumogallion complex in natural waters, Analyst 126 (2001) 698-702.

[19] (a) A. K. Singh, V. K. Gupta and B. Gupta, Anal. Chim. Acta 585 (2007) 171-178;
(b) J.B. Vincent, Nutr. Rev. 58 (2000) 67-72.

[20] S. Latva, J. Jokiniemi, S. Peraniemi and M. Ahlgren, J. Anal. At. Spectrom., 18 (2003) 84-86.

[21] R. McRae, P. Bagchi, S. Sumalekshmy, C. J. Fahrni, Chem. Rev. 109 (2009) 4780-4827.

[22] R. A. Anderson, Chromium, Trace Elements in Human and Animal Nutrition; Academic:New York, NY, 1987.

[23] T. O'Brien, H.G. Mandel, D.E. Pritchard, S.R. Patierno, Critical role of chromium (Cr)-DNA interactions in the formation of Cr-induced polymerase arresting lesions, Biochemistry 41 (2002) 12529-12537.

[24] A. Zhitkovich, G. Quievryn, J. Messer, Z. Motylevich, Reductive activation with cysteine represents a chromium(III)-dependent pathway in the induction of genotoxicity by carcinogenic chromium(VI), Environ. Health Perspect. 110 (2002) 729-733.

[25] J.B. Vincent, Quest for the molecular mechanism of chromium action and its relationship to diabetes, Nutr. Rev. 58 (2000) 67-72.

[26] (a) P.Ghosh, P. K. Bharadwaj, S. Mandal, S. J. Ghosh,Ni(II), Cu(II), and Zn(II) Cryptate-Enhanced Fluorescence of a Trianthrylcryptand: A Potential Molecular Photonic OR Operator, Am. Chem. Soc. 118 (1996) 1553-1554;

(b) M. Royzen, Z. Dai, W. J. Canary, Ratiometric Displacement Approach to Cu(II) Sensing by Fluorescence, J. Am. Chem. Soc. 127 (2005) 1612-1613;

(c) K. Rurack, M. Kollmannsberger, U. Resch-Genger, J. Daub,A Selective and Sensitive Fluoroionophore for HgII, AgI, and CuII with Virtually Decoupled Fluorophore and Receptor Units, J. Am. Chem. Soc. 122 (2000) 968-969;

(d) S. Banthia, A. Samanta, A New Strategy for Ratiometric Fluorescence Detection of Transition Metal Ions, J. Phys. Chem. B 110 (2006) 6437-6440;

(e) L. Prodi, F. Bolletta, M. Montalti, N. Zaccheroni, Luminescent chemosensors for transition metal ions, Coord. Chem. Rev. 205 (2000) 59-83;

(f) N. B. Sankaran, S. Banthia, A. Das, A. Samanta, Fluorescence signaling of transition metal ions: a new approach, New J. Chem. 26 (2002) 1529-1531;

(g) B. Ramachandram, A. Samanta, Modulation of metal–fluorophore communication to develop structurally simple fluorescent sensors for transition metal ions, Chem. Commun. (1997) 1037-1038.

[27] T. Keawwangchai, N. Morakot and B. Wanno, Fluorescent sensors based on BODIPY derivatives for aluminium ion recognition: an experimental and theoretical study, J. Mol. Model 19 (2013) 1435-1444.

[28] T. Shamspur, I. Sheikhshoaie, M.H. Mashhadizadeh, Flame atomic absorption spectroscopy (FAAS) determination of iron(III) after preconcentration on to modified analcime zeolite with 5-((4-nitrophenylazo)-N-(2′,4′-dimethoxyphenyl))salicylaldimine by column method, J. Anal. Atom. Spectrom. 20 (2005) 476–478

[29] P. Vanloot, B. Coulomb, C. Brach-Papa, M. Sergent, J.-L. Boudenne, Multivariate optimization of solid-phase extraction applied to iron determination in finished waters, Chemosphere 69 (2007) 1351–1360.

[30] V.K. Gupta, A.K. Singh, M.R. Ganjali, P. Norouzi, F. Faridbod, N. Mergu, Comparative study of colorimetric sensors based on newly synthesized Schiff bases, Sens. Actuators B 182 (2013) 642–651.

[31] G.J. Park, H.Y. Jo, K.Y. Ryu, C. Kim,A new coumarin-based chromogenic chemosensor for the detection of dual analytes Al^{3+} and F^{-}, RSC Adv. 4 (2014) 63882–63890.

[32] M. Ghaedi, S.Y.S. Jaberi, S. Hajati, M. Montazerozohori, M. Zarr, A. Asfaram, L.K. Kumawat, V.K. Gupta, Preparation of iodide selective carbon paste electrode with modified carbon nanotubes by potentiometric method and effect of cus-nps on its response, Electroanalysis 27 (2015) 1516–1522.

[33] M. Sperling, S. Xu, B. Welz, Determination of chromium(III) and chromium(VI) in water using flow injection on-line preconcentration with selective adsorption on activated alumina and flame atomic absorption spectrometric detection, Anal. Chem. 64 (1992) 3101–3108.

[34] V.K. Gupta, A.K. Jain, P. Kumar, S. Agarwal, G. Maheshwari, Chromium(III)-selective sensor based on tri-o-thymotide in PVC matrix, Sens. Actuators. B 113 (2006) 182–186.

[35] J. Miao, L. Wang, W. Dou, X. L. Tang, Y. Yan, W. S. Liu, Tuning the selectivity of two chemosensors to Fe(III) and Cr(III), Org. Lett. 9 (2007) 4567- 4570.

[36] (a)A. Ghorai, J. Mondal, S. Chowdhury, G.K. Patra, Solvent-dependent fluorescent-colorimetric probe for dual monitoring of Al^{3+} and Cu^{2+} in aqueous solution: an application to bio-imaging, Dalton Trans. 45 **(**2016) 11540-11553;

(b) A. Ghorai, J. Mondal, S. Bhattacharya, G.K. Patra, A 'chromogenic' and 'fluorogenic' bis-Schiff base sensor for rapid detection of hydrazine both in solution and vapour phases, Anal. Methods 7(2015) 10385-10393;

(c) A. Ghorai, J. Mondal, R. Chandra, G.K. Patra, A reversible fluorescent-colorimetric chemosensor based on a novel Schiff base for visual detection of CO_3^{2-} in aqueous solution, RSC Adv. 6 (2016) 72185-72192.

[37] (a) A.K. Manna, K. Rout, S. Chowdhury, G.K. Patra, A dual-mode highly selective and sensitive Schiff base chemosensor for fluorescent colorimetric detection of Ni^{2+} and colorimetric detection of Cu^{2+}, Photochem. Photobiol. Sci.18 (2019) 1512-1525;

(b) A.K. Manna, S. Chowdhury, G.K. Patra, A novel hydrazide-based selective and sensitive optical chemosensor for the detection of Ni^{2+} ions: applications in live cell imaging, molecular logic gates and smart phone-based analysis, Dalton Trans. 48 (32), 12336-12348; (c) J. Mondal, A. K. Manna and G. K. Patra, Inorg. Chim. Acta 474 (2018) 22-29;

(d) A. K. Manna, J. Mondal, R. Chandra, K. Rout, G. K. Patra, J. Photochem. Photobiol, A: Chem. 356 (2018) 477-488.

[38] SMART & SAINT Software Reference manuals, version 5.0; Bruker AXS Inc.: Madison, WI, (1998).

[39]T. Gruene, H. W. Hahn, A. V. Luebben, F. Meilleur, G. M. Sheldrick, Refinement of macromolecular structures against neutron data with SHELXL 2013, J. Appl. Cryst., 47 (2014) 462-466.

[40] L. J. Farrugia, WinGX suite for small-molecule single crystal crystallography, J. Appl. Crystallogr. 32 (1999) 837-838.

[41] A.D. Becke, Density-functional thermochemistry. III. The role of exact exchange, J. Chem. Phys. 98 (1993) 5648-5652.

[42] C. Lee, W. Yang, R.G. Parr, Development of the Colle-Salvetti correlation-energy formula into a functional of the electron density, Phys. Rev. Sect. B, 37 (1988) 785-789.

[43] R. Nandhini, G. Venkatachalam, M. D. Kumar, M. Jaccob, Dinuclear Pd(II) complexes containing bis-O,N-bidentate Schiff base ligands: Synthesis, characterization, DFT study and application as Suzuki–Miyaura coupling catalysts, Polyhedron 158 (2019) 183–192

[44] D. E. Crawford, C. K. G. Miskimmin, A. B. Albadarin, G. Walker and S. L. James, Organic synthesis by Twin Screw Extrusion (TSE): continuous, scalable and solvent-free, Green Chem. 19 (2017) 1507–1518.

[45] I. Kaabi, L. Sibous, T. Douadi, S. Chafaa, X-ray structure of a new ligand: Di[(4-phenylimino) 4-diethyl salicylaldehyde] ether and electrochemical study of its copper (II) and cobalt (II) complexes, J. Mol. Str. 1084 (2015) 216-222.

[46] L. Xu, Y. Kim, S.J. Kim, 3,5,3′,5′-Tetra-methyl-N,N′-bis-(salicyl-idene)bi-phenyl-4,4′-di-amine, Acta Cryst. 61 (2005) 03344-03345.

[47] A. K. Manna, J. Mondal, K. Rout, G.K. Patra, A new ICT based Schiff-base chemosensor for colorimetric selective detection of copper and its copper complex for both colorimetric and fluorometric detection of Cysteine, J. Photochem. Photobiol A: Chem. 367 (2018) 74-82.

[48] D. Jiang, X. Yang, X. Zheng, L. Bo, T. Zhu, H. Chen, L. Zhang, S. Huang, Self-assembly of luminescent 12-metal Zn–Ln planar nanoclusters with sensing properties towards nitro explosives, J. Mater. Chem. C, 6 (2018) 8513-8521.

[49] A. Barba-Bon, A. M. Costero, S. Gil, M. Parra, J. Soto, R.Martı´nez-Ma´-n˜ez, F. Sanceno´n, A new selective fluorogenic probe for trivalent cations, Chem. Commun. 48 (2012) 3000-3002.

[50] S. Goswami, K. Aich, A. K. Das, A. Manna, S. Das, A naphthalimide–quinoline based probe for selective, fluorescence ratiometric sensing of trivalent ions, RSC Adv. 3(2013) 2412-2416.

[51] M. Venkateswarulu, T. Mukherjee, S. Mukherjee, R. R. Koner, Turn-on trivalent cation selective chemodosimetric probe to image native cellular iron pools, Dalton Trans. 43 (2014) 5269-5273.

[52] J. Wang, Y. Li, N. G. Patel, G. Zhang, D. Zhou, Y. Pang, A single molecular probe for multi-analyte (Cr^{3+}, Al^{3+} and Fe^{3+}) detection in aqueous medium and its biological application, Chem. Commun. 50 (2014) 12258-12261.

[53] S. Paul, A. Manna, S. Goswami, A differentially selective molecular probe for detection of trivalent ions (Al^{3+}, Cr^{3+} and Fe^{3+}) upon single excitation in mixed aqueous medium, Dalton Trans. 44 (2015) 11805 -11810.

[54] R. Alam, R. Bhowmick, A.S.M. Islam, A. Katarkar, K. Chaudhuri, M. Ali, A rhodamine based fluorescent trivalent sensor (Fe^{3+}, Al^{3+}, Cr^{3+}) with potential applications for live cell imaging and combinational logic circuits and memory devices, New J. Chem. 41 (2017) 8359-8369.

- Two salicylaldimine-functionalized dipodal *bis* Schiff base chemosensors **L1** and **L2** have been developed for detection of Al^{3+} and Cr^{3+}
- They have fairly low detection limits and high association constants.
- The binding stoichiometries have been confirmed as 2:2 by ESI-MS, ^{1}H NMR and Job's plot.
- These chemosensors find application in colorimetric test kits and real sample analysis.

Graphical Abstract

Simple salicylaldimine-functionalized dipodal *bis* Schiff base chromogenic and fluorogenic chemosensors for selective and sensitive detection of Al^{3+} and Cr^{3+}

Rukhmani Chandra, Amit Kumar Manna, Meman Sahu, Kalyani Rout and Goutam K. Patra*

Department of Chemistry, Guru Ghasidas Vishwavidyalaya, Bilaspur (C.G)

Two salicylaldimine-functionalized ether based dipodal *bis* Schiff base low cost fluorescent colorimetric chemosensors **L1** and **L2** have been designed and synthesized. These sensor could simultaneously detect Al^{3+} and Cr^{3+} by change in both absorption and fluorescence intensity in CH_3CN-H_2O (1/1, v/v). The detections limits of the sensor **L1**, for Al^{3+} ($1.73x10^{-7}$M) and Cr^{3+}($1.12x10^{-7}$M) and of the sensor **L2**, for Al^{3+}($4.34x10^{-7}$M) and Cr^{3+}($7.73x10^{-7}$M) are far below than the limit set by the World Health Organization (WHO) for drinking water. These chemosensors find application in colorimetric test kits and real sample analysis.

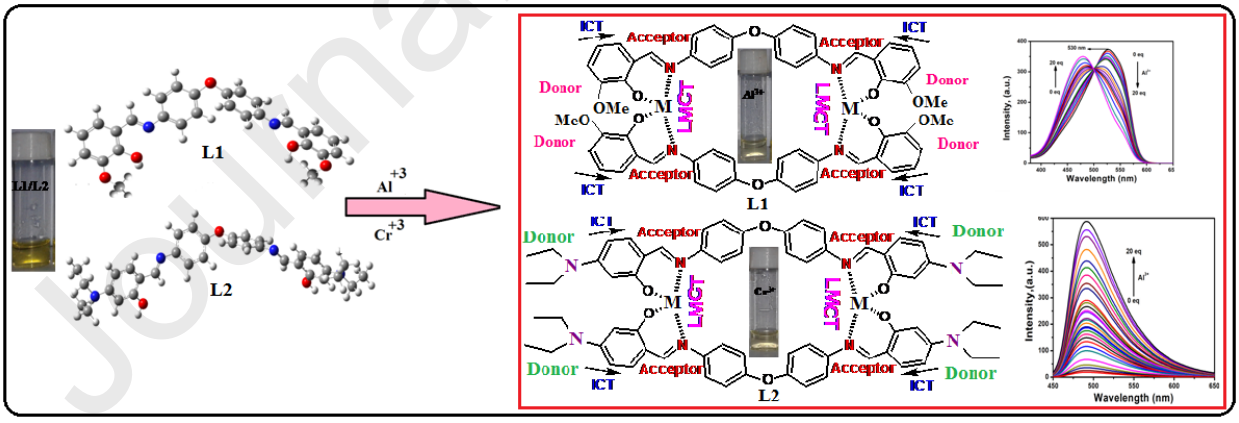

.

Simple salicylaldimine-functionalized dipodal *bis* Schiff base chromogenic and fluorogenic chemosensors for selective and sensitive detection of Al^{3+} and Cr^{3+}

Rukhmani Chandra, Amit Kumar Manna, Meman Sahu, Kalyani Rout and Goutam K. Patra*
Department of Chemistry, Guru GhasidasVishwavidyalaya, Bilaspur (C.G)

Conflict of Interest: The authors declare no conflict of interest.